1968

Fast neutron induced resistivity changes in order-disorder Fe_3Al

Bruce A. Betts

Department: Mining and Nuclear Engineering

FAST NEUTRON INDUCED RESISTIVITY CHANGES IN ORDER-DISORDER Fe_3Al

BY 758
BRUCE ALLAN BETTS, 1938

A

THESIS

submitted to the faculty of the

UNIVERSITY OF MISSOURI - ROLLA

in partial fulfillment of the work required for the

Degree of

MASTER OF SCIENCE IN NUCLEAR ENGINEERING

Rolla, Missouri

1968

Approved by

H. P. Leighly Jr. (Advisor) D. Ray Edwards

J. Flanders

ABSTRACT

Resistivity measurements were made of ordered, disordered and intermediate states of order-disordered specimens of Fe_3Al while being irradiated by neutrons.

All the specimens were irradiated at ambient temperature, approximately 35°C in a modified Bulk Shielding Swimming Pool type reactor. The ordered and near ordered specimens increased in resistivity indicating disordering whereas the disordered and near disordered specimens decreased in resistivity indicating an ordering process was occuring. By extrapolation, an equilibrium condition was determined and estimated at 130-135 micro-ohms-cm resistivity at a dose of 1.02×10^{20} n/cm^2. This is the estimated resistivity that would remain constant during irradiation because the ordering and disordering affects of neutron irradiation would be in equilibrium.

The temperature effect was very pronounced during the initial hour or two of reactor operation as indicated by the high damage rates incurred during this period ($5 - 20 \times 10^{-15}$ $\frac{\text{micro-ohms-cm}}{\text{neutron/cm}^2}$). After initial period was passed the damage rate dropped to $0.5 - 5 \times 10^{-15}$ $\frac{\text{micro-ohms-cm}}{\text{neutron/cm}^2}$.

ACKNOWLEDGEMENTS

The author wishes to express his deepest appreciation to Dr. H. P. Leighly, Jr., Associate Professor of Metallurgical Engineering, for his most helpful assistance, guidance and patience throughout this stimulating research investigation.

He also wishes to thank Dr. D. R. Edwards, Director of the Nuclear Reactor for his timely suggestions and cooperation and also to Alva E. Elliot and the late John N. Sturgeon for their assistance, cooperation, and time in operating the reactor.

The author wishes to thank Mr. William Buehler of the Naval Ordnance Laboratory for the iron-aluminum alloy he so willingly supplied.

TABLE OF CONTENTS

LIST OF ILLUSTRATIONS

Figures Page

LIST OF TABLES

CHAPTER I

INTRODUCTION

This investigation was undertaken to determine the effects of neutron irradiation on the electrical resistivity of ordered, disordered and intermediate ordered state of Fe_3Al. The change in electrical resistivity is taken as being a direct measure of the state of order of the alloy.

From this data it was hoped that an ordered-disordered state could be found that would show no change in electrical resistivity while undergoing neutron irradiation and possibly some postulation made as to the mechanism for the change in electrical resistivity brought about by neutron irradiation.

The source of neutrons for this experiment is to be a BSR type "swimming pool" reactor, located on the campus of the University of Missouri - Rolla, Rolla, Missouri. Electrical resistance measurements are to be made using a double precision Kelvin bridge and the measurements made while the specimens were being irradiated. Temperature was held at approximately 30 to 35°C by means of a gaseous nitrogen flow around the specimen at all times.

Resistance measurements were made at approximately one hour intervals and these later were converted over to electrical resistivity and plotted against total neutron dose as a means of evaluating the results. The resistivity values were converted into the order parameter S from

Muto's[8] relationship, and plotted against total neutron dose for further evaluation.

CHAPTER II

REVIEW OF LITERATURE

This review will deal with those areas of literature that are of greatest importance to the research project. They are: superlattice structure, effects of neutron irradiation on electrical resistivity and the measurement of the long range order parameter as a function of neutron dose.

A. Superlattice Structure

Guy[2] defines a crystal as "the regular arrangement of atoms in a solid in a three-dimensional pattern". The three-dimensional network of imaginary lines connecting these atoms is called the space lattice, while the smallest unit having the full symmetry of the crystal is called the unit cell. According to Avner[3] the specific unit cell for each metal is defined by its parameters which are the edges of the unit cell a,b,c and the angles α (between b and c), β (between a and c) and γ (between a and b).

Often the lattice points (points of intersection of the imaginary lines) are composed of an array of atoms instead of a single atom. However, no matter which it is, each lattice point has the identical surroundings(4). That is to say the surrounding atomic array looks exactly the same when viewed from any lattice point. Also of importance is that the structure will not be quite regular if the atoms making up the lattice are not of the same relative size. Different size atoms tend to displace each other which is an

important factor in superlattice formation.

Superlattice as defined by Reed-Hill[5] is when the atoms in an alloy arrange themselves in a predetermined, stable configuration that extends through large regions of the crystal. When this occurs, a state of long range order is said to exist and the resulting structure is called a superlattice or superstructure.

In order to understand this phenomenon it must be recalled that the x-ray scattering factor (reflectivity) of atoms of different elements increases directly with the atomic number, and in the alloy Cu_3Au, which can be used as an example of a superlattice alloy, if the atoms are ordered in a manner similar to that shown in Figure 1, then the two x-ray beams shown in the right in this figure, whose paths differ by one half of the wave length λ, will not cancel as they would if all the atoms were alike but produce an additional line on an x-ray plate. The unit cube for this order structure is shown in Figure 2.

In the ordered state of this particular alloy, the gold atoms occupy the corner lattice sites and the copper the face centered sites of the face-centered cubic lattice. Each corner atom of gold is shared by eight adjacent unit cells and since there is a total of 8 gold atoms per unit cell it means that effectively each unit cell has one (1) gold atom, $\left[\frac{1}{8} \times 8 = 1\right]$. Each face-centered lattice site is occupied by a copper atom and is only shared by one other unit cell so the total number of copper atoms per unit cell is 3, $\left[\frac{1}{2} \times 6 = 3\right]$. This accounts for the compound Cu_3Au.

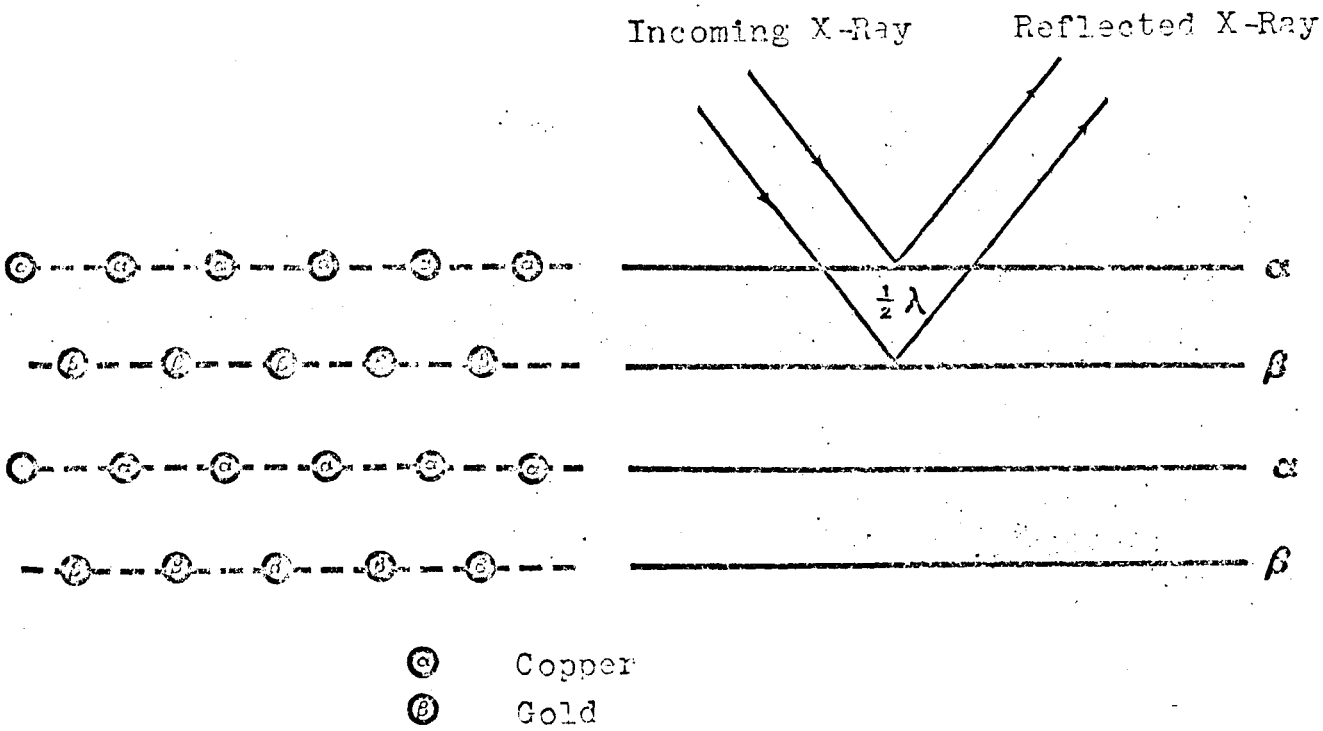

Figure 1. X-Ray Reflectivity of Ordered Cu_3Au.

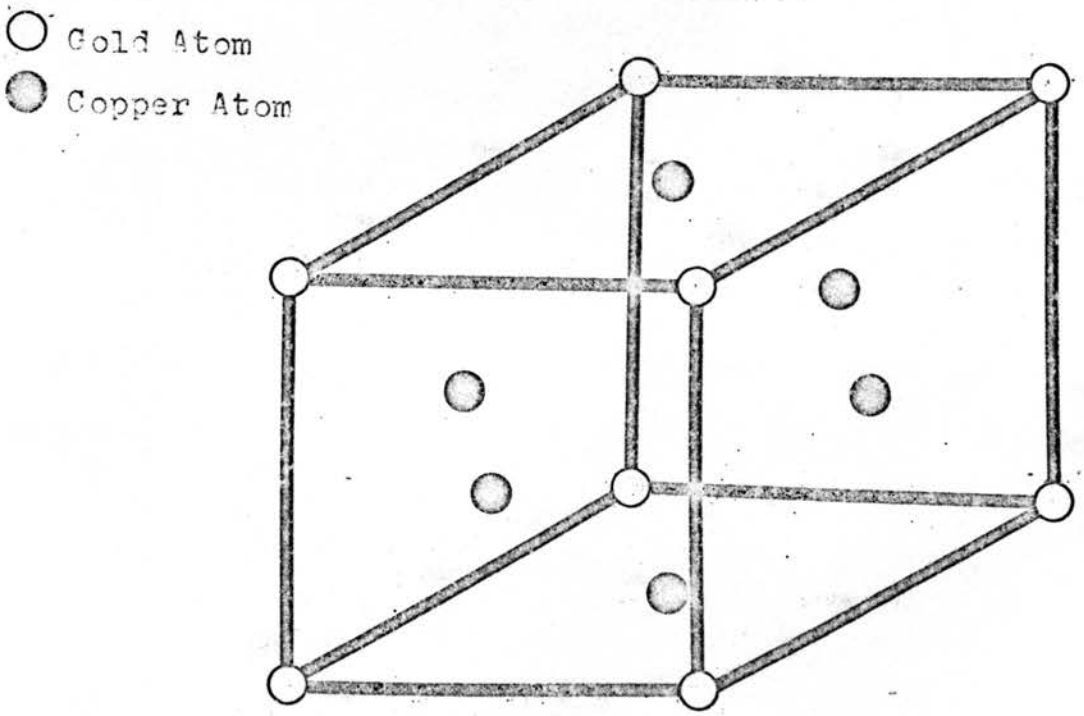

Figure 2. Ordered Cu_3Au Unit Cell.

Figure 3 shows the lattice structure of the ordered Fe_3Al alloy, the alloy under investigation. This alloy is body-centered cubic with iron atoms at the four corners of the cube. Each corner atom is shared by 8 unit cells thereby each cell has one iron atom $\left[\frac{1}{8} \times 8 = 1\right]$ for the corner position. Iron atoms also occupy the mid-points of each of the 12 edges and is shared by four unit cells giving a unit cell 3 more iron atoms (1/4 x 12 = 3). More iron atoms occupy the six face-center position and are shared by two unit cells adding three more atoms of iron to the unit cell (1/2 x 6 = 3). Finally there are 5 iron atoms wholly in the interior of the unit cell thus giving a total of 12 (1 + 3 + 3 + 5) iron atoms per unit cell. There are four aluminum atoms all occupying interior positions in the unit cell which gives a 3:1 ratio of iron to aluminum atoms accounting for the stoichiometric compound Fe_3Al.

The iron atoms mentioned above are located, according to Miller indicies nomenclature, at the (0,0,0), (1/2,0,0), (0,1/2,0), (0,0,1/2), (0,1/2,1/2), (1/2,0,1/2), (1/2,1/2,0), (1/2,1/2,1/2), (1/4,1/4,1/4), (1/4,3/4,3/4), (3/4,1/4,3/4) and (3/4,3/4,1/4). The aluminum atoms are located at (3/4,3/4,3/4), (3/4,1/4,1/4), (1/4,3/4,1/4), and (1/4,1/4, 3/4). Application of the crystal structure factor equation to the Fe_3Al superlattice reveals that superlattice reflections will occur for planes whose indices are either all odd or all even and whose sum is not a multiple of 4. The principal lattice reflections, i.e., those not contingent upon atomic order, have Miller indices twice those occuring

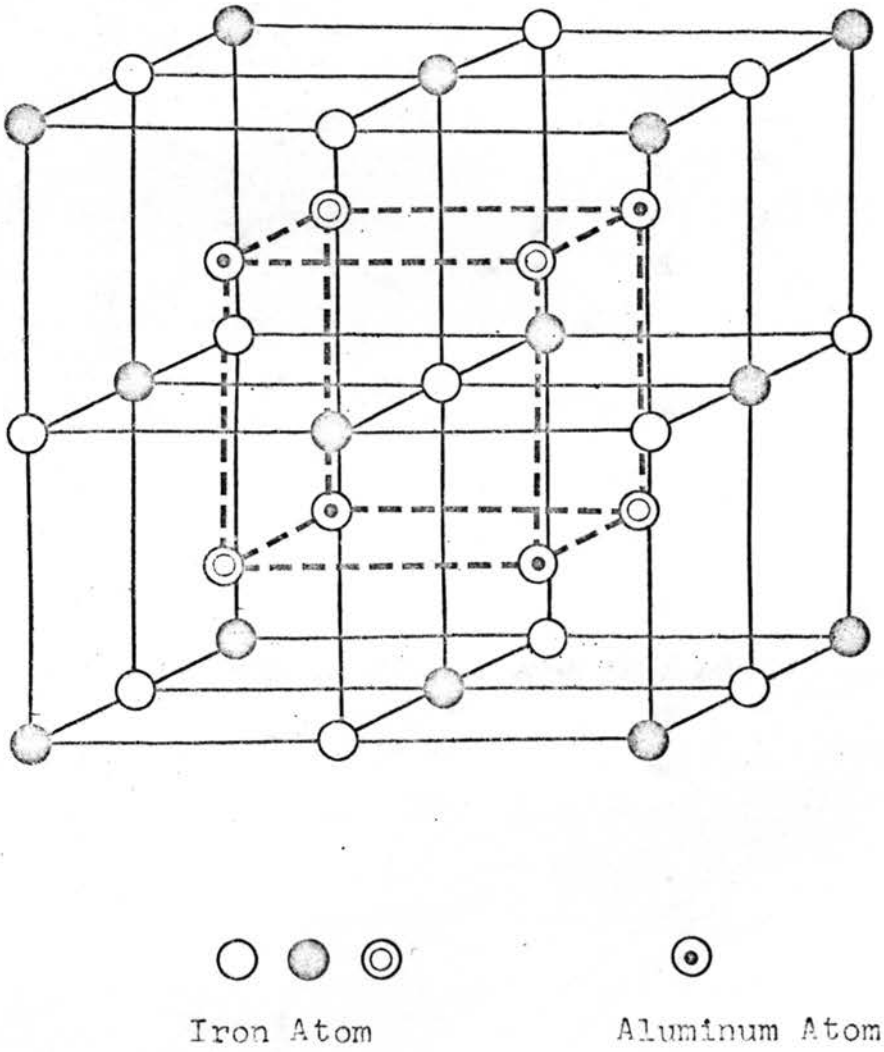

Figure 3. Ordered Fe_3Al Unit Cell.

in α iron because eight unit cells of body-centered cubic symmetry are required to define the Fe_3Al structure[19].

The Miller indices of the principal and superlattice lines of the three cubic structures occuring in iron-rich Fe-Al solid solutions are given in Table I. The Fe_3Al superlattice presupposes the presence of FeAl order, of which it is a further development. It is therefore impossible to have a finite (111) intensity without having a finite (200) intensity, but the converse is not true. The intensity of these two lines convey two distinct kinds of information. Reference to Figure 3 shows that the (200) line is sensitive only to the distribution of aluminum atoms between the centers and corners of the small unit cells, and therefore indicates the extent of development of FeAl order. The (111) line is sensitive only to the distribution of the aluminum atoms among four of the eight cube centers of each group of eight small cells which make up the Fe_3Al unit cell.

TABLE I

Indices of Main Lines and Superlattice Lines* For the Structures of Fe-Al Solid Solutions From Bradley and Jay (1)

Random Structure	Fe Al Structure	Fe_3Al Structure
110	100*	111*
200	110	200
211	111*	220
220	200	311*
	210*	222
310	211	400
	220	331*
	300*	420
	310	422
		333*
		440
		531
		600
		620

T. Muto and Y. Takagi[8] discuss the manner in which some physical value can be assigned to the state to which an alloy is ordered. This is needed as not all alloys are wholly ordered or disordered under all conditions but lie somewhere between. This function is called the ordering parameter and is designated by S for long-range order and σ for short range order.

Long range order means the regular geometrical array of atoms at the lattice site is extended over many atomic distances and calculations take into account the effects of atoms at rather large atomic distances away from another atom. Short range order takes into account only the nearest neighbor atoms for the forces acting on the atom and therefore relates itself to only a short atomic distance relationship.

To calculate the long-range order parameter the Bragg and Williams[9] method can be used, on a binary alloy. When the perfectly ordered arrangement of atoms in binary alloys is realized, the lattice sites occupied by A atoms will be called α sites and those by B atoms β sites. Consider now a binary alloy Fe_3Al having a body centered cubic structure, the position of the iron atoms as previously mentioned become α sites and those at the aluminum atoms β sites, respectively. The total number of atoms, which is also the total number of atom sites, is represented by N. F_A shall be designated as the fraction of Fe atoms and $F_\beta = 1-F_A$ the fraction of Al atoms. The fraction of α sites occupied by Fe atoms (right atoms) is termed r_α. The fraction of α

sites wrongly occupied (by Al atoms) is $\omega_\alpha = 1 - r_\alpha$. Similarly, r_β and $\omega_\beta = 1 - r_\beta$ represent the rightly and wrongly occupied β sites, respectively. The number of Fe atom on β sites is therefore $\omega_\beta F_\beta N$ and is equal to the number of Al atoms on α sites, $\omega_\alpha F_A N$. Then the Bragg-Williams order parameter or long-range order parameter S may be written as:

$$S = \frac{r_\alpha - F_A}{1 - F_A} = \frac{r_\beta - F_\beta}{1 - F_\beta} \qquad (1)$$

which is defined so that it is unity for perfect order and zero for perfect disorder.

A new order parameter introduced by Bethe[10], the short range order σ , is different from long range order S in not being connected with the α and β sites but with the configuration of the nearest neighbors. Let $\mathcal{Q}$ be the total number of pairs in the lattice and each atom surrounded by Z nearest neighbors. Then we have:

$$Q = \left(\frac{Z}{2}\right) N \qquad (2)$$

where N is the number of lattice sites.

If the number of pairs, which are Fe-Fe, Al-Al and Fe-Al be denoted by $\mathcal{Q}_{Fe-Fe}$, $\mathcal{Q}_{Al-Al}$, $\mathcal{Q}_{Fe-Al}$, the fraction of pairs which are unlike is:

$$q = \frac{Q_{Fe-Al}}{Q} \qquad (3)$$

In the state of perfect order, q has a maximum value of q_m (which is unity for simple cases), and for the disordered state a smaller value q_r. Bethe's short range order σ is defined by:

$$\sigma = \frac{q - q_r}{q_m - q_r} \qquad (4)$$

so that the limits unity and zero are obtained for perfect order and randomness in a way similar to the case of long-range order S.

The short range order σ measures the way in which, on the average, each atom is surrounded by its neighbors or the extent of local order, in contrast to the long-range order S which gives the order upon the α and β sites over the entire lattice. The short-range order σ, therefore, is not uniquely determined by the long-range order S. In fact, for perfect long-range order (S = 1), the short-range order must also be perfect (σ = 1), but it is possible to have no long-range order at all but still have some short-range order.

Temperature has the greatest effect on ordered alloys. By heating the alloy Fe_3Al above the critical temperature, which causes disordering of the alloy, and holding it above this critical temperature, the amount of ordering present then becomes directly related to the rate of cooling to room temperature. A fast quench gives random placement of the atoms or a disordered structure. Slow cooling at a rate of approximately 25°C/HR for Fe_3Al, gives a completely ordered structure. Cooling rates greater than 25°C/HR and slower than quenching give structures with degrees of ordering related to rate of cooling.

Bradley and Jay[1] found in iron-aluminum alloys of 0-50

atom per cent aluminum quenched from 600 to 700°C, that the distribution of the aluminum atoms was random in the range 0 to 25 atom per cent aluminum; i.e., no superlattice was detected. In the range 25 to 50 atom per cent aluminum, a superlattice was found even though the alloys were quenched. It was noted that at 25 atom per cent where, upon increasing the aluminum content, the structure changes from disordered to ordered, there is also a discontinuous decrease in the lattice parameter. Here is direct evidence that the ordered arrangement provides a better fit of the atoms and hence a more dense structure.

Phase diagram work has been done on iron-aluminum alloys by various researchers. From work done by Bradley and Jay[1], Hansen and Anderko[11] have postulated for the solid solution region in iron-aluminum alloys the phase diagram shown in Figure 4. In this diagram the phase represented by α'' is a DO_3 superlattice structure derived from stoichiometric Fe_3Al. This superlattice structure is shown in Figure 3.

Taylor and Jones,[12] from precision lattice parameter measurements over a broad range of temperatures and composition, and McQueen and Kuczynski,[13] from differential dilatometric heating curves of several alloys, have proposed equilibrium diagrams. These are shown together in Figure 5. Sykes and Banpfylde,[14] while studying various physical properties of iron-aluminum alloys, found, as one would expect, that the electrical resistivities of alloys containing from 2 to 12 weight per cent aluminum were uneffected

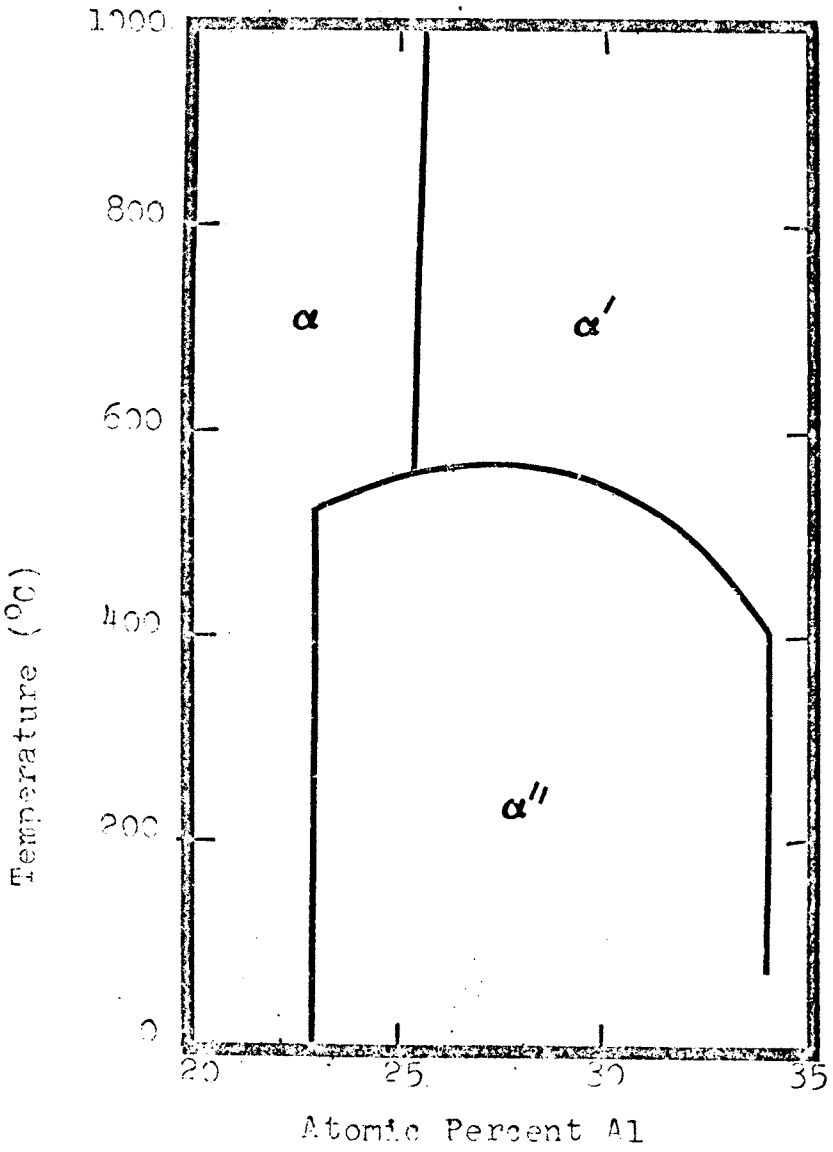

Figure 4. Iron Aluminum Equilibrium Diagram. Determined by Hansen and Anderko(11).

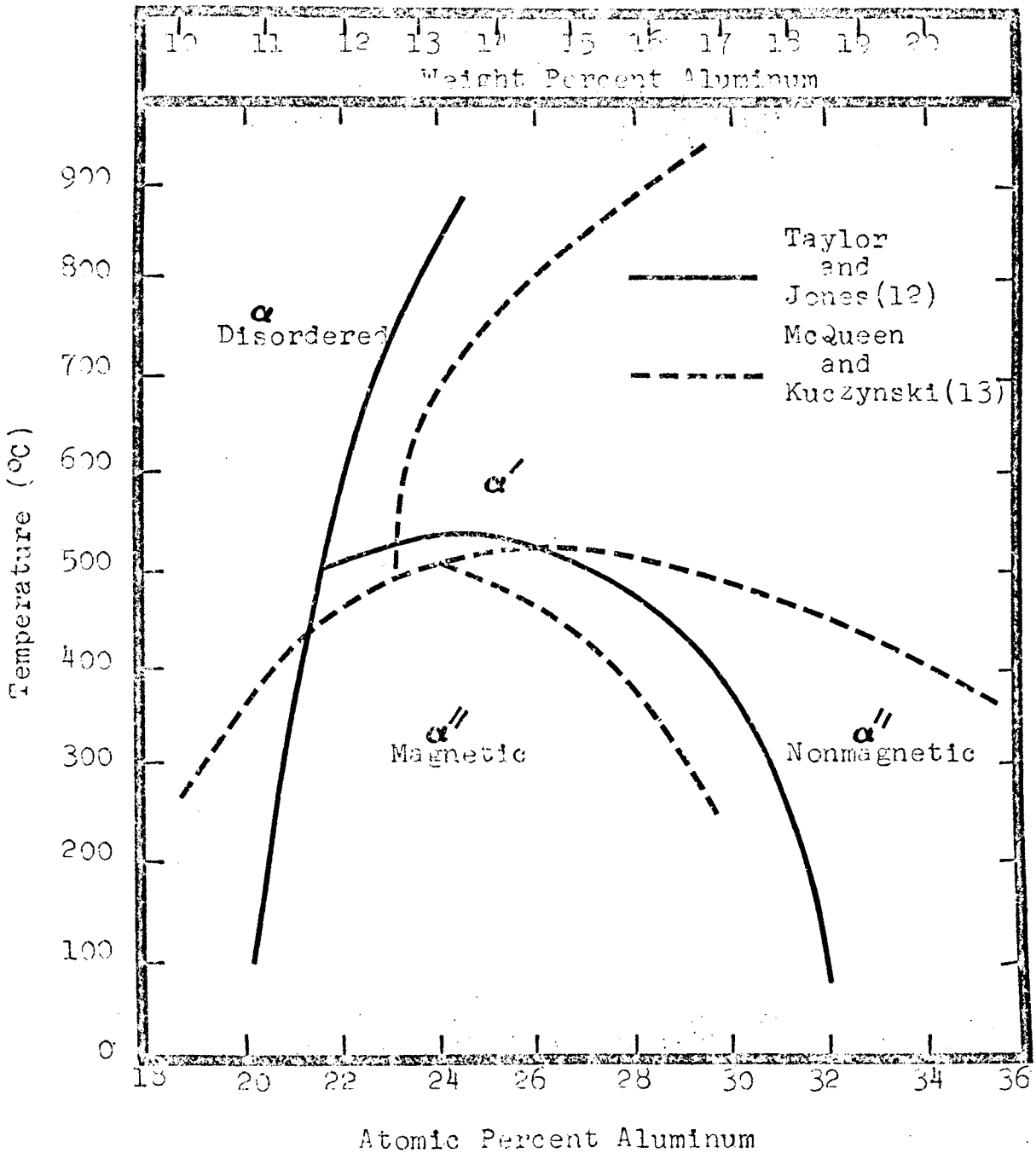

Figure 5. Constitution Diagram of Iron-Rich Fe-Al Alloys in the Solid Solution Range.

by heat treatments. However, they found that alloys containing from 12 to 16 weight per cent aluminum underwent a remarkable change in resistivity when slow cooled from high temperatures. The maximum effect occuring at approximately 14 weight per cent aluminum, corresponding to stoichiometric Fe_3Al, represented a difference of approximately 50 per cent between the resistivities of specimens quenched from 700°C and those slow cooled from 700°C.

Bennet[15] studied the effects of heating and cooling rates on the electrical resistivity for various iron-aluminum alloys. The findings of his study of Fe_3Al are shown in Figure 6. This graph shows a change in curvature for both alloys at the Curie point, 625°C and between 400 and 560°C. The change in resistivity in the 400 to 560°C range is surmized by Bennet to be boundary effects between ordering nuclei.

In a kinetics study by McQueen and Kuczynski[13] on the ordered alloy Fe_3Al they determined the long range order parameter, S, from Muto's[8] equation

$$S = \sqrt{\frac{\rho_d - \rho}{\rho_d - \rho_o}} \qquad (5)$$

where ρ_d is the resistivity of the disordered alloy, ρ_o the resistivity of the ordered alloy and ρ, the resistivity of the specimen being examined. The results of this portion of their investigation is shown in Figure 7 where the long range order parameter, S, is shown versus temperature. The accuracy of this determination is limited by the fact that the value of ρ_d used corresponds to the maximum Fe-Al disorder

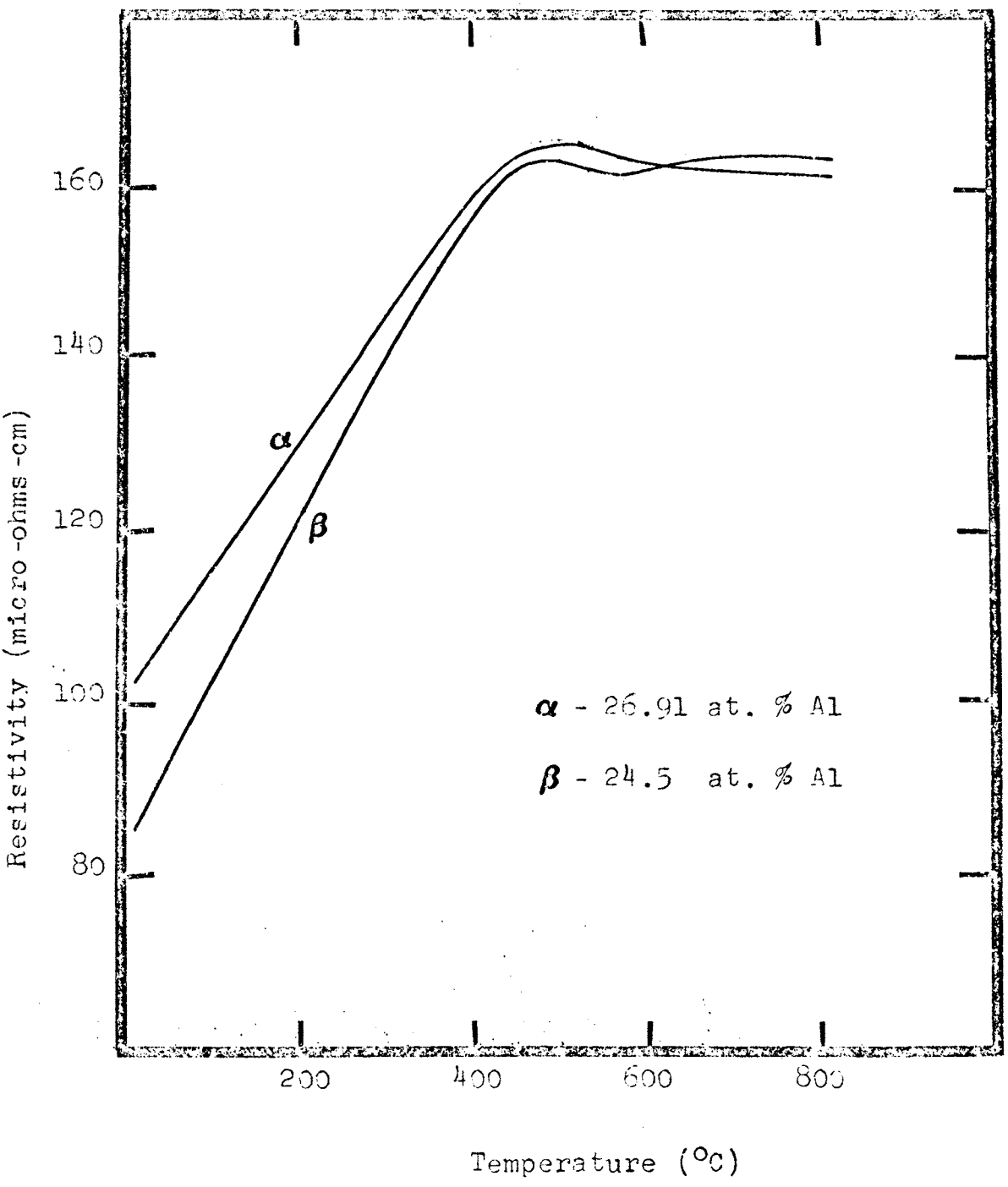

Figure 6. Resistivity vs. Temperature Curves on Slow Cooling (in Equilibrium) for Two Fe-Al Alloys as Determined by Bennett(15).

obtainable in an alloy of composition corresponding to Fe_3Al and does not represent a completely disordered alloy, because of the presence of the Fe_3Al B2 type order occuring even after quenching from temperatures above the critical point.

Rauscher[18] investigated the effect of temperature on resistivity of iron-aluminum alloys in order to determine a general outline of the atomic ordering process. The results of the slow cooling process are shown in Figure 7 and agree very closely with those of Bennet. Rauscher also conducted x-ray diffraction measurements of the superlattice line intensities from single crystals of Fe_3Al to determine the relative long range Fe_3Al order parameters as a function of temperature. From this investigation he concluded that the Fe_3Al orders in a manner similar to that predicted by the Bragg-Williams theory of superlattice transformation. A change in S was found by Rauscher from $S = 0.45$ at 530°C to $S = 0$ at 550°C. This is shown in Figure 8. This rapid drop in S implies that the critical temperature is somewhere near 540°C for Fe_3Al.

Some other X-ray work has been done on the alloy by Lawley and Cahn[16] and Shmueli and Rudman[17]. Lawley and Cahn's investigation was in the area of high temperature x-ray diffraction studies of ordering in iron-aluminum alloys. They calculated the absolute values of the long range order parameter, S, for the alloys containing 24.8 and 25.5 atomic per cent aluminum from superlattice line intensity measurements. They found the maximum value of S (at room temperature) to be 0.80 for the 24.8 atom per cent aluminum alloy

and 0.75 for the 25.5 atom per cent aluminum alloy. The critical temperature for the Fe_3Al superlattice in these alloys were determined to be 540°C and 542°C respectively. Shmueli and Rudman's investigation was in the field of x-ray studies of long range order as a function of quenching temperature. They used alloys containing 25 and 29 atom per cent aluminum. The maximum degree of long range Fe_3Al order attainable in the stoichiometric Fe_3Al composition was found to be $S = 0.83$. The maximum order achieved in the 29 atom per cent aluminum alloy corresponded to $S = 0.65$. The critical temperatures were found to be 558°C in the case of stoichiometric Fe_3Al alloy and 545°C in the alloy with higher aluminum content.

B. Neutron Irradiation Effects

We will consider for the most part only fast neutrons (>1 Mev) in our discussion. The following discussion is taken largely from Dienes and Vineyard[20], Billington and Crawford[21], Bishay[22], Penkovskii[23], and Toma[24].

The major damage caused by neutron bombardment on nonfissile material is to displace atoms as a result of a collision. A secondary effect is to produce tranmutations in the nuclei. The amount of irradiation a material receives is dependent upon the flux in the reactor position in which its placed. The flux is defined as the number of neutrons per cubic centimeter (or unit volume) times the velocity of the neutron. In the cgs system the flux dimension is neutrons/cm^2 - sec or may be thought of as the number of neutrons passing through a unit area in a unit

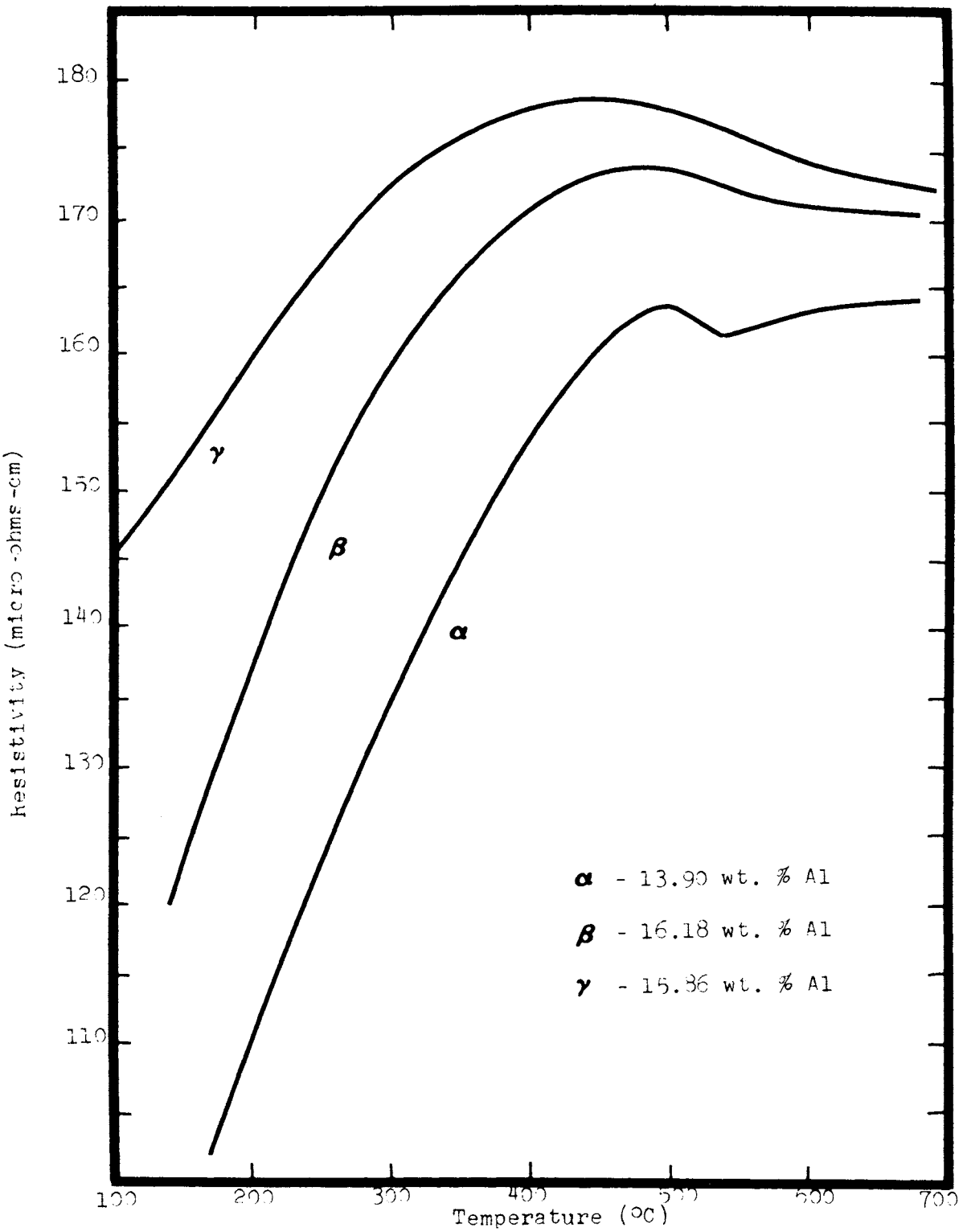

Figure 7. Resistivity vs. Temperature upon Slow Cooling of Fe-Al Alloys as Determined by Hauscher(18)

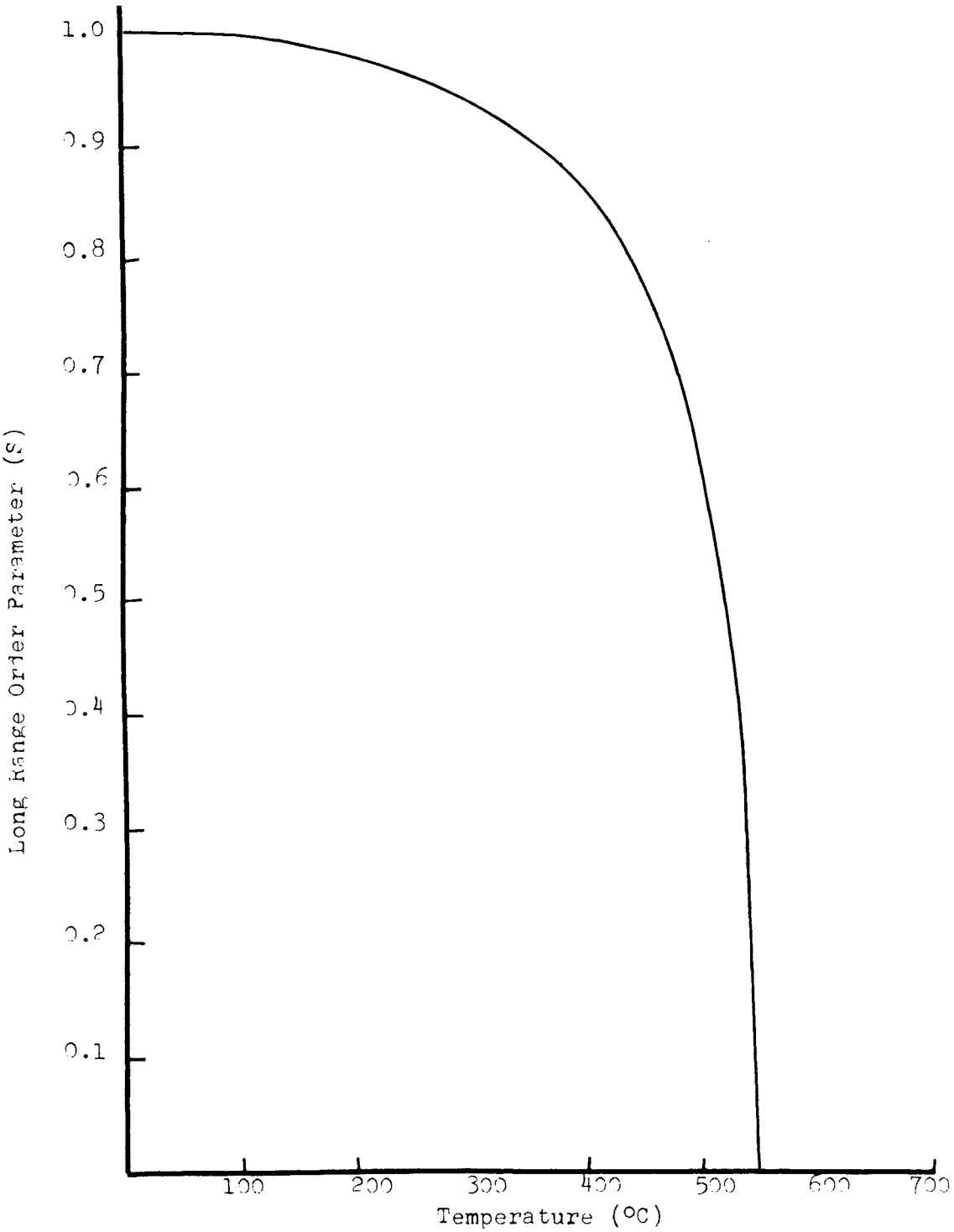

Figure 8. Equilibrium Long Range Order Parameter as a Function of Temperature as Determined by Rauscher(18).

time in any direction.

In most reactors the neutron flux is somewhere in the range of 10^{10} to 10^{14} neutrons/cm^2 - sec. Toma[24] in his work stated that the cross section of an atom was approximately $10^{-15} cm^2$, and each atom would have a neutron pass through it about once every 15 seconds. The reason the neutron is able to pass through the atom is that it is electrically neutral thereby not being effected the electron cloud or the positive charged nucleus. For the most part neutrons pass completely through the lattice without a single collision or absorption and are lost as far as the specimen is concerned.

Collisions do occur and when they do, the atom is usually displaced from its lattice site and lodged in an interestitial position. The probability of an absorption occuring instead of scattering is considerably less and depends upon the capture cross section of the material which varies with the energy of the incoming neutron, whereas the probability of scattering is almost a constant.

The probability of a collision between the neutron and the nucleus has the units of "barns". A "barn" being equal to $10^{-24} cm^2$. The average cross section for fast neutron scattering is of the order of 5 barns. Therefore the rate at which scattering takes place is based on the equation $R = \phi \sigma$ where R is the rate of scatter, ϕ is the neutron flux and σ is the scatter cross section. Assuming a reactor neutron flux equal to 10^{12} neutrons/cm^2 sec. and a scatter cross section of 5 barns gives a scatter rate, $R = 5.40^{-12}$ scatters/nuclei-sec.

When a collision occurs the fast neutron (1 - 2 Mev energy range) imparts some of its energy to the target nucleus thereby causing it to be "knocked" from its lattice site. The energy given up during this collision comes from the equation found in elementary mechanics books. The conservation of energy and momentum limit the maximum kinetic energy E_{max} that a neutron of mass M_1 and initial energy E can give to a nucleus of mass M_2 to:

$$E_{MAX.} = \frac{4 M_1 M_2}{(M_1 + M_2)^2} E \qquad (6)$$

This is for a strictly head-on collision. For collisions other than head-on the average value of energy transferred is 1/2 E_{max}. For aluminum, the value of E_{max} for a 2 Mev neutron is 0.28 Mev, while for iron E_{max} is 0.14 Mev.

For most materials the average energy imparted to an atom upon collision with a fast neutron is significantly higher than the threshold energy E_t necessary for it to be displaced from its lattice position. The average value for E_t is approximately 25 ev. therefore most collisions with fast neutrons result in the atom being displaced from its lattice site.

The atom that has been displaced by the collision is called a "primary knock-on" and travels at a speed approximately 100 times faster than the speed of sound in the given material. Since its velocity and energy are large, the lattice forces are unimportant and the ion penetrates the material as if it were a dense gas.

The fast ion, created by a fast neutron collision

carries a positive charge and therefore interacts with the electrons and nuclei which it comes into close contact with. The electrostatic forces due to the lattice atoms are of a sufficient magnitude as to slow this ion down in a short distance and time, therefore, the effect of the primary knock-on is in a very small area near to the initial collision area.

However, the greater mass of the ion causes it to move slower than an electron of the same energy, thereby raising the question whether the moving ion has sufficient speed to excite electrons. If an electron in an atom makes a large number oscillations during the time the ion travels through the atom, it absorbs little energy from the ion. This is because the energy gained during the inward swing of an oscillation is largely lost during the outward swing. It can be concluded then that except for extremely fast primary knock-on ions the electrons are usually not excited. Also it can be concluded that the primary knock-on travels as a positively charged ion rather than a bare nucleus again except in the case of extremely high velocity and energy knock-ons. A rough criterion for whether the electrons move with the nucleus or not is that those electrons with less energy than the primary knock-on will be left behind.

Present interpretation of the changes in the properties of solids brought about by high energy neutron irradiation centers around the production of several types of defects in the solid by the radiation. These defects are:

a) vacancies, b) interstitial atoms, and c) impurity atoms. Each of these simple defects are described briefly below.

a) Vacancies. Vacant lattice sites may be created by collisions of energetic neutrons with the atom in a solid lattice. The energy transferred in these collisions is usually sufficient for the recoiling atom to create further vacant lattice sites by subsequent collisions. Thus, for each primary collision a cascade of collisions resulting in vacancies and interstitials. This is shown in Figure 9.

b) Interstitial atoms. The atoms that are displaced from their equilibrium positions in the lattice will stop in a interstitial, or non equilibrium position, provided they do not recombine immediately with a nearby vacancy. This also is shown in Figure 9.

c) Impurity atoms. Impurity atoms are formed under neutron bombardment by transmutation. A special case of this is the introduction of fission products by the fission process. The effect of fission fragments is usually more pronounced than that of neutron-induced transmutation, although both mechanisms are often insignificant compared to other radiation effects.

In addition to simple collisions there are other important processes leading to observable radiation effects. They are d) replacement collisions, e) thermal and displacement spikes f) focusing collisions and g) crowdions. These processes may be described briefly as follows:

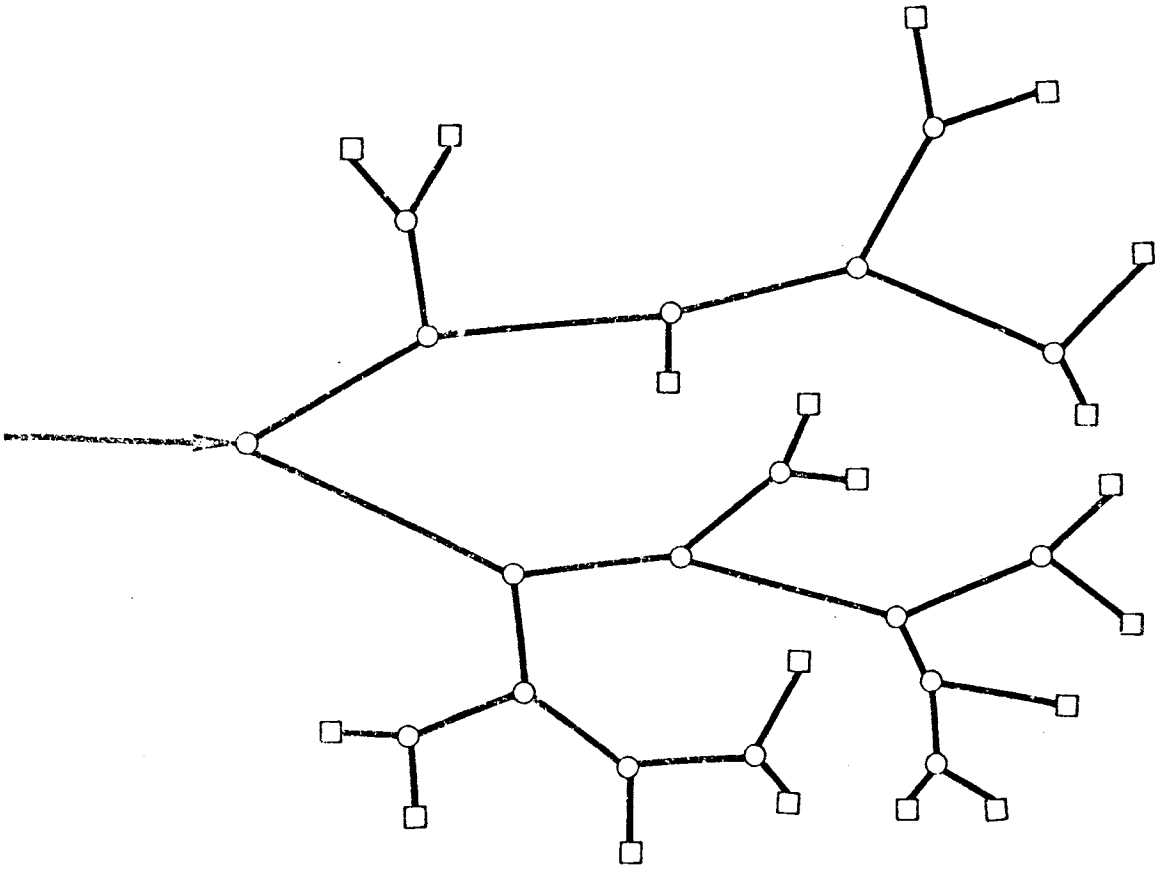

□ Interstitial Atom

○ Vacancy

Figure 9. A Cascade of Displacements Produced by a Fast Ion.

d) Replacement collisions. If a collision between a moving interstitial atom and a stationary atom results in the ejection of the stationary atom and leaves the interstitial with insufficient kinetic energy for it to escape from the vacancy it has created, then this atom will fall into the vacancy, dissipating its kinetic energy through the lattice vibrations as heat. Calculations show that for a reasonable choice of energy parameters the number of replacement collisions may exceed the number of displacement collisions. The result is the interchange of moving atoms with lattice atoms, which, can lead to observable effects especially in ordered alloys.

e) Thermal and displacement spikes. A fast particle moving through a lattice, or an atom that has been hit just hard enough to vibrate with large amplitude without being displaced, will rapidly transfer energy to its neighbors, which become abnormally excited. Thus a region of material around the track of the fast moving particle or knock-on atom will be heated to a high temperature. The region of excitation expands rapidly, and at the same time there is a drastic decrease in temperature. The result is called a thermal spike, i.e., rapid heating and quenching of a small volume of material. Calculations indicate that the duration of a high temperature of approximately $1000^{\circ}K$ in a region involving some thousands of atoms might be 10^{-10} to 10^{-11} seconds. When the energy of the fast moving atom falls below a transisition value (which depends on the atomic number) the mean free path between displace-

ment collisions becomes of the order of atomic spacing. Then each collision results in a displaced atom, and the end of the trail is believed to be a region containing of the order of one-to-ten-thousand atoms in which local melting and turbulent flow have occurred a very short time interval. This is called a displacement spike and is shown schematically in Figure 10.

f) Focusing collisions. Silsbee[25] suggested that an atom dislodged as a result of an initial collision can produce further displacements in a given direction, namely, in one of the directions of closest packing of the atoms. In this case, the atom dislodged by the secondary collision is displaced at a smaller angle to the given direction than the first atom, and itself displaces a third atom from the lattice, and so on. The displacements occur at a progressively smaller angle to the given direction the displaced atoms are, as it were, "focused" in this direction. This is shown in Figure 11 for a face centered cubic lattice. The conditions for the existance of such a "focusing of displacements" are as follows:

$$\frac{d}{r_0} \leq 2 \sin \beta \qquad (7)$$

where d is the interatomic distance; r_0 is the radius of the metal atom: β is the angle of displacement of the atom relative to the closest packing. For small values of β Equation 7 becomes:

$$\frac{d}{r_0} \leq 2 \qquad (7a)$$

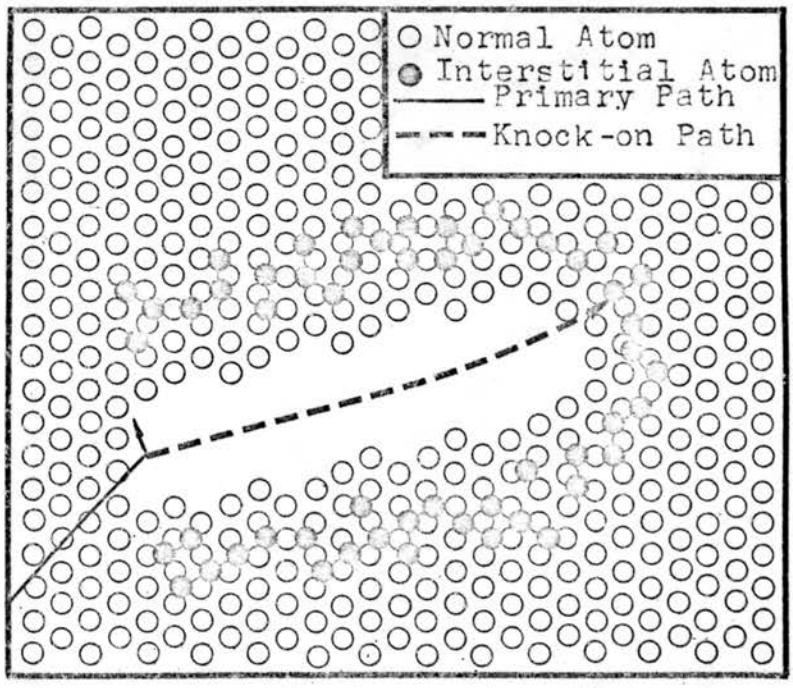

Figure 10. Picture of a Displacement Spike as Determined by Brinkman(29).

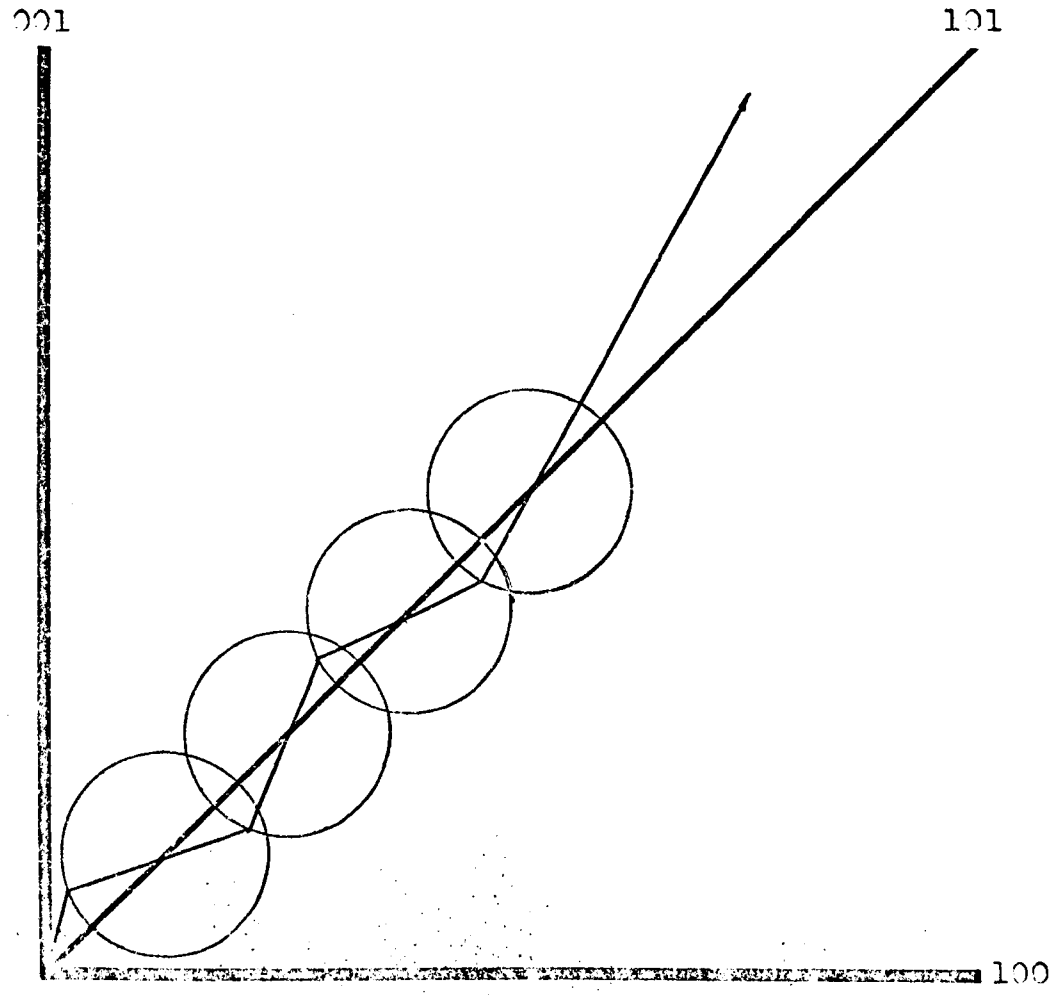

Figure 11. Schematic of Focusing Collision.

According to this model, thermal spikes in the metal lattice can be "diffused" along the direction of closest packing of the atoms. A quantitative evaluation of displacements, according to Silsbee, shows the threshold of displacement of the atom to be 50 ev. i.e., twice the value found by other investigators. However, even these calculations show the validity of the application of the billard ball model to collisions of atoms with fast particles or among themselves.

The focusing effect is normally weaker in an atomic row not characterized by close packing. Thus, according to Leibfried[26], the preferential directions of focusing of atomic displacements will also be the directions of closest packing. These directions in a face-centered cubic lattice, are the [110] or [101] directions only.

g) Crowdions. This phenomenon is also referred to as defocusing. The other extreme of focusing is when $\frac{d}{r} \geq 2$. In this case the energy is rapidly defocused, even though θ_o may be very close to zero. Conditions for this type of collision are shown in Figure 12. Provided this initial energy transferred into the row is sufficiently large, these conditions lead to the production of an interstitial, i.e., an atom is ejected from the close-packed row at some distance from the initial impact within the row. Hence, such a correlated collision may indeed be visualized as a dynamic crowdion.

C. Neutron Effects on Order-Disorder Alloys.

In an ordered alloy, anytime an atom is displaced from

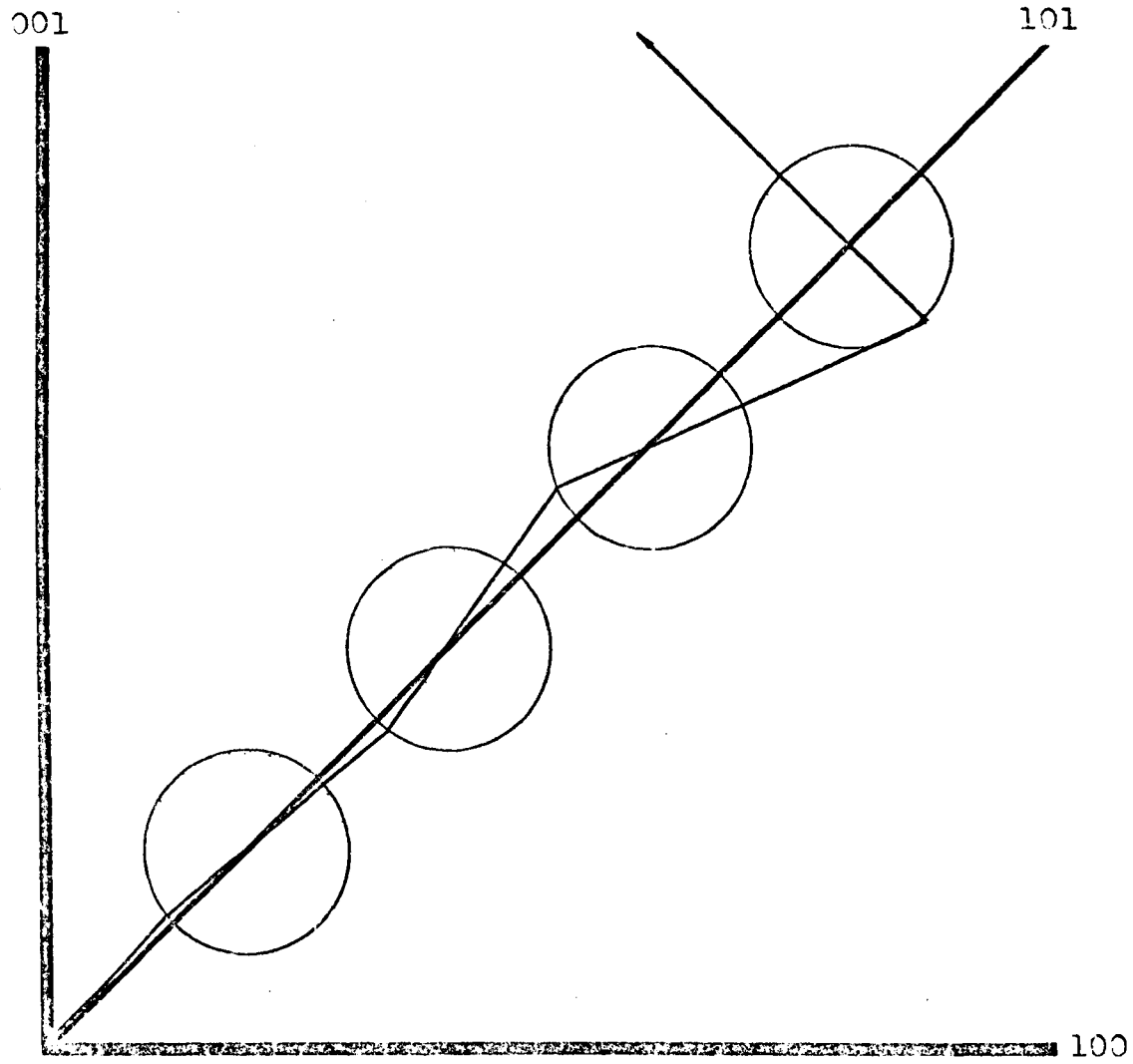

Figure 12. Schematic of Dynamic Crowdions (Defocusing).

its original lattice site to an interstitial position or fills a vacancy, there is a change in the degree of ordering unless it falls into a lattice vacancy that should be occupied by the same kind of atom. The likelihood of the latter occuring is considerably less than the previously mentioned choices.

Considerable research in the effects of radiation on copper-gold alloys has been carried out[26,27,28,29,30]. In most cases the means of measuring the effects was by the change in resistivity of the alloy. Siegel[26] observed that the resistivity of Cu_3Au in the ordered state became progressively higher with room-temperature neutron irradiation, while samples in the disordered state showed no change other than a slight increase due to transmutations. The supposition that the increase in resistivity meant a decrease in the amount of order was confirmed by x-ray measurements of the superlattice lines.

Utilizing Seitz' method of calculating defect concentration, Siegel found that the disordering introduced by the irradiation was in excess of that to be expected simply on the basis of displacements. He found that it was necessary to use the thermal spike concept for an adequate explanation. While this experiment lends some credibility to the thermal spike concept, it has since been shown by Kinchin and Pease[30] that a modification of Seitz' calculations employing the replacement concept will adequately explain the data.

H. L. Glick et al.[31,32] have shown that bombardment at 80°C with neutrons will cause an initially ordered sample to

show at first a slight drop in resistance succeeded by a rapid increase, reaching a value approximately 30% above the original value at an integrated exposure of 6×10^{19}. The initial resistivity was 5.2 micro-ohms-cm whereas a resistivity of 4.7 micro-ohm-cm or less is considered appropriate for annealed Cu_3Au in the ordered state. The original decrease is not easily explained, but it implies that the crystal was initially not in equilibrium either because of a departure from perfect order or because of the retention of a non-equilibrium number of defects (probably vacancies). The irradiation then causes the metastability to be erased with an attendant decrease in resistivity.

Another part of the same experiment consisted of following the resistivity charge in an initially disordered sample irradiated at the same time and temperature. The resistivity dropped steadily and finally saturated at a value 7% below the original value. Presumably the rates of the opposing reactions are essentially balanced at this value and temperature. This latter experiment confirmed the observations by Blewitt and Coltman[33], that the resistivity of disordered samples in substantially reduced by irradiation, provided that the temperature of irradiation is above room temperature. Blewett and Coltman observed much larger decreases than reported above. This might be attributed to the higher temperature of irradiation (150 and 200°C instead of 80°C), or to the fact that the 80°C irradiation was carried out at 10^{13} neutrons/cm^2 sec. In addition, it was seen that there was a time lag of approximately 12 hours

before the resistance decrease stopped after the irradiation was stopped, indicating a relaxation time for ordering of 12 hours at 200°C. In the absence of irradiation, this time would be thousands of hours.

Saenko[34] investigated the change in resistivity brought on by neutron irradiation at 80°C of both ordered and disorder Fe_3Al. Measurements of the crystal lattice parameters and the intensity of the superlattice lines were also made as a function of neutron irradiation. He examined both the Fe_3Al-DO_3 type and the Fe_3Al-B2 type. The Fe_3Al-DO_3 type having greater long range order than the Fe_3Al-B2.

After irradiation to 3×10^{18} neutrons/cm^2, the intensity of the superlattice lines is sharply reduced in the x-ray pattern $\left(I(111)_\alpha / I(220)_\beta \approx 0.02\right)$. Further increase in the integrated neutron exposure results in the complete disappearance of these lines.

As can be seen in Table II and Figure 13, the electrical resistivity and the crystal lattice parameter of the alloy is the annealed (Fe_3Al - DO_3) and the quenched (Fe_3Al-B2) states become almost equivalent. This suggests that the irradiation of the specimens which initially had different atomic distributions should result in the formation of similar physical states.

In checking this idea a study of the graph in Figure 14 was made. Here samples of specimens in the annealed-irradiated and annealed-unirradiated states and specimens in the original-irradiated and original-unirradiated states were subjected to various annealing temperatures and their

TABLE II

Electrical Resistivity Change of the Fe_3Al Alloy During Neutron Irradiation at 80°C.(34)

Treatment of Alloy	Electrical Resistivity (μ ohms cm)				
	Initial Condition	After Irradiation Exposure			
		3×10^{18} (n/cm^2)	1.5×10^{19} (n/cm^2)	7×10^{19} (n/cm^2)	1.35×10^{20} (n/cm^2)
Annealing at 560-250°C in 12 hours	108.0	111.5	120.5	129.0	140.0
Oil Quenched from 750°C	153.4	149.5	145.0	141.0	138.0

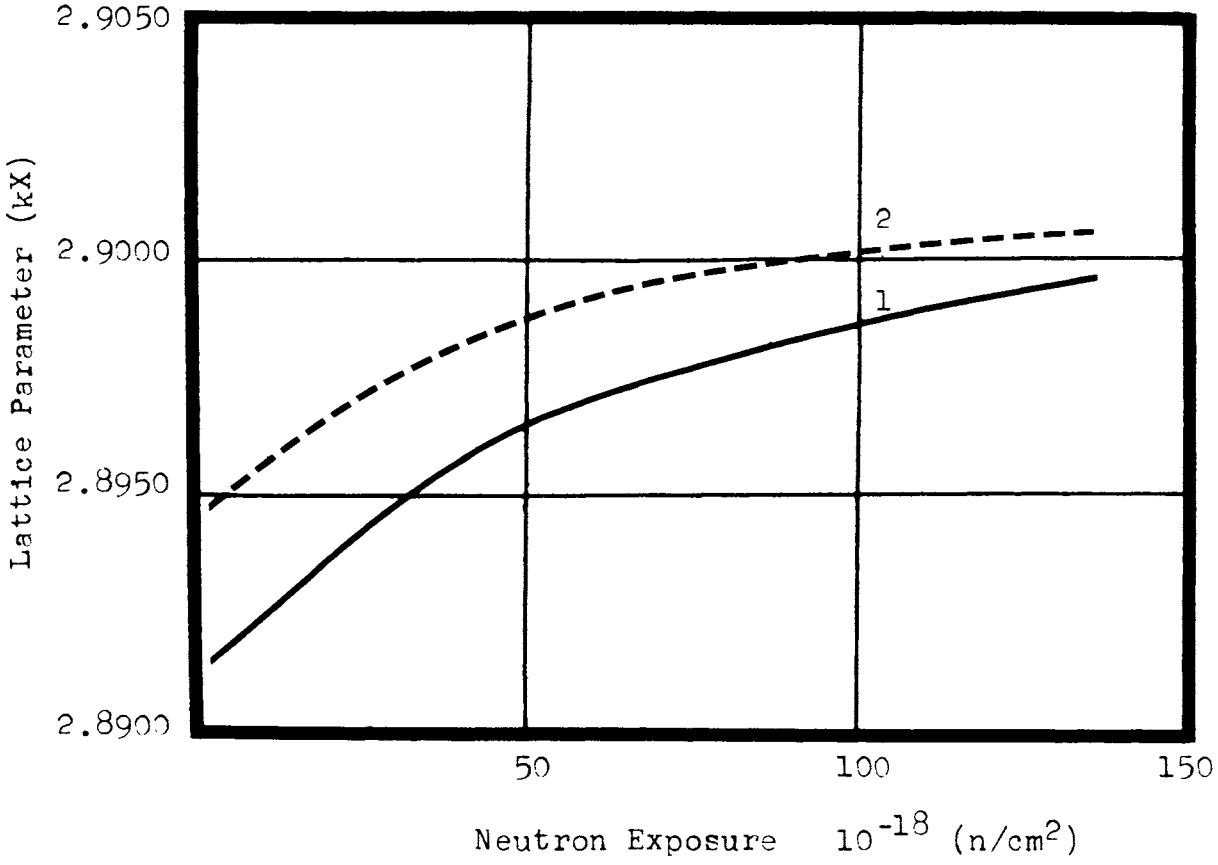

Figure 13. The Effects of the Irradiation Exposure on the Crystal Lattice Parameter of Fe_3Al. 1.) Annealed (500-250°C 12 hrs); 2.) Oil Quenched (from 750°C) as Determined by Saenko(34).

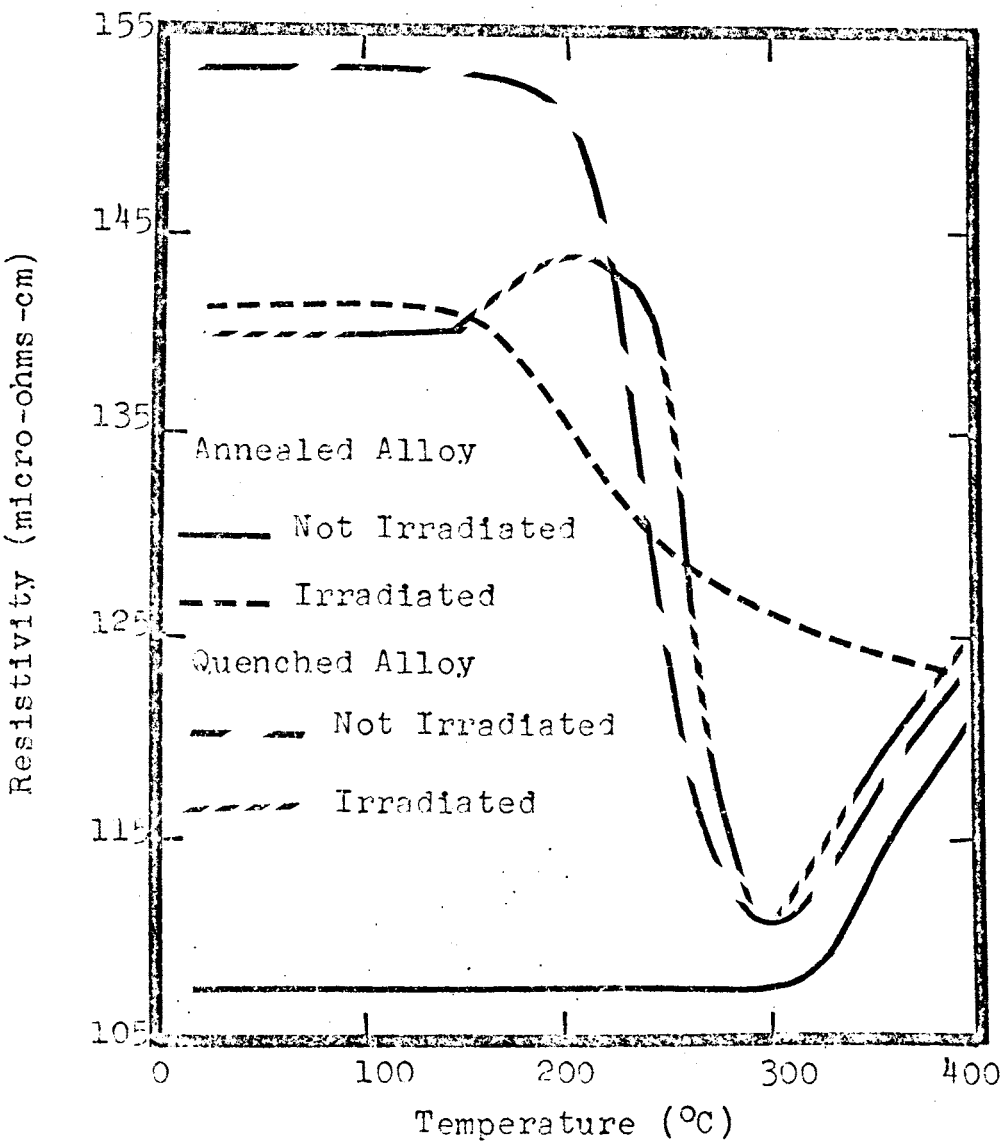

Figure 14. Variation of the Resistivity of Annealed and Quenched Fe_3Al, Both in the Initial State, and After Irradiation by a dose of 1.35×10^{20} n/cm^2 During the Process of Isochronal Annealing as Determined by Saenko(34).

electrical resistance recorded.

A temperature versus resistance study of the irradiated specimen did not confirm the suggestion concerning the similar nature of the physical states formed in the quenched and annealed alloys as a result of the neutron irradiation. Moreover, the initial course of the resistance points to a tendency of each alloy to regain its initial state which existed before irradiation.

Using Saenko data from Table II and plotting a graph of resistivity versus exposure yields Figure 15. Here we see the tendency that leads to the previous suggestion that the two initial states approach a common state. Saenko concluded from his investigation that neutron exposure at about 80°C destroys the order distributions of heterogeneous atoms existing in the Fe_3Al alloy subjected to two different heat treatments, one ordered, the other disordered. Also irradiation in a high neutron flux does not give rise to profound structural changes of the alloy. The state formed is metastable.

Lastly he suggested that a hypothesis concerning the radiation disordering of the non fissionable alloy through displacement spike formation does not appear to apply to the present case. It is thought that the experimental data might be understood on the basis of Kinchen and Pease's theory concerning the radiation-induced formation of displacements and replacements. The effective disordering may also take place as a result of replacements forming during focusing collisions.

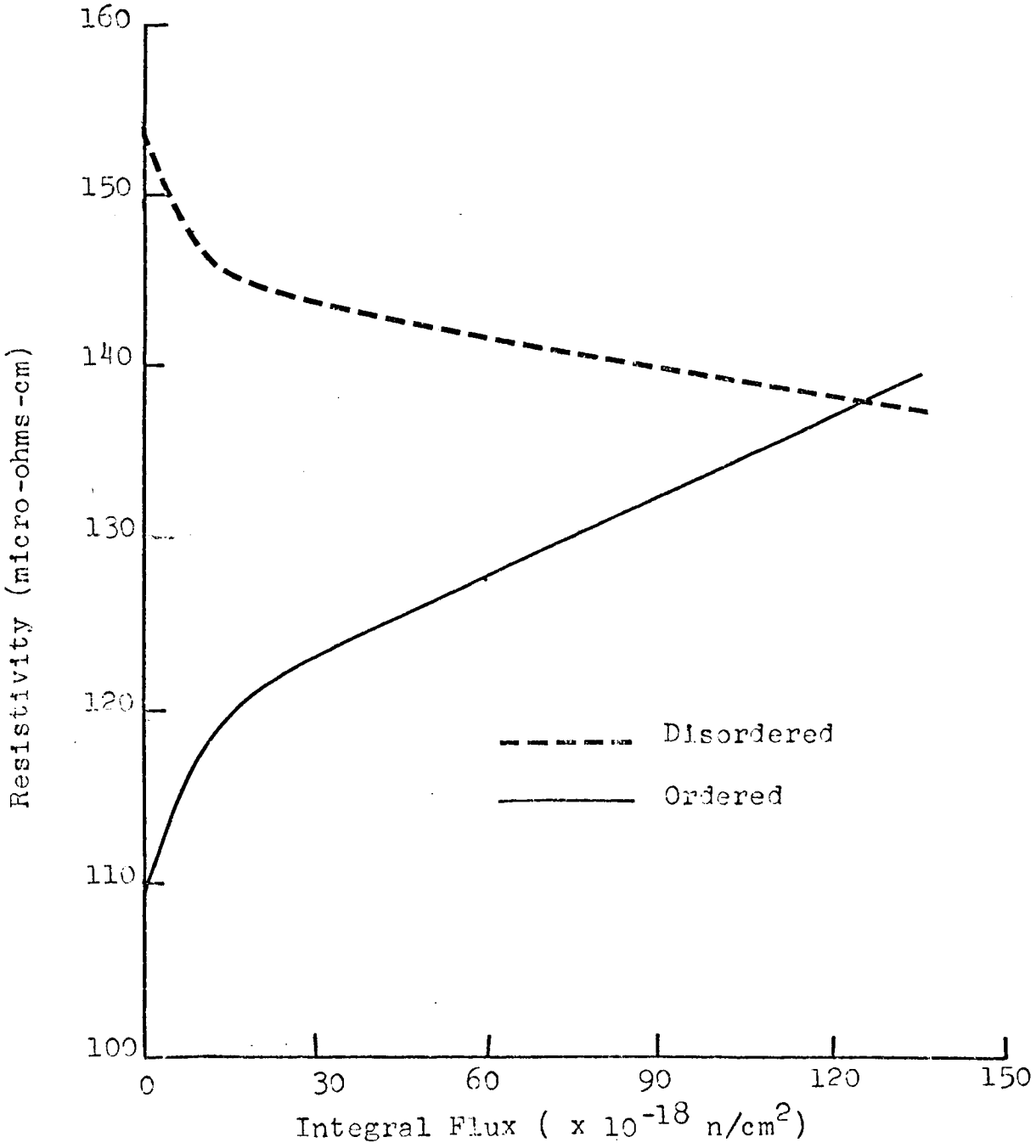

Figure 15. Dependence of the Resistivity of Preliminarily Ordered and Disordered Fe_3Al on the Flux as Determined by Saenko(34).

Toma investigated the effects of neutron irradiation on Fe_3Al but at elevated temperatures (100°C to 300°C at 50°C intervals). In his investigation flat strip specimens of ordered or disordered alloy were used. The results of his investigation are shown in Figure 16, plotted as Muto's relationship order parameter[5] versus temperature for both the completely ordered and completely disordered states. The order parameter S, is determined by Muto's relationship as found in (8).

Toma found a large decrease in ordering with irradiation. This is found by the fact that the order parameter for the ordered specimen decreased as temperature increases at a constant dose. Perfect order has an order parameter S of 1.0 whereas the completely disordered state has an order parameter S of 0.0.

He concludes that the disordering increases as a result of the production of displacement spikes and replacement collisions which disrupt the long range order in the lattice. Also he states that the vacancy/interstitial pairs and interstitials produced by replacement collisions are metastable at the elevated temperatures for the order is increased as the temperature is lowered.

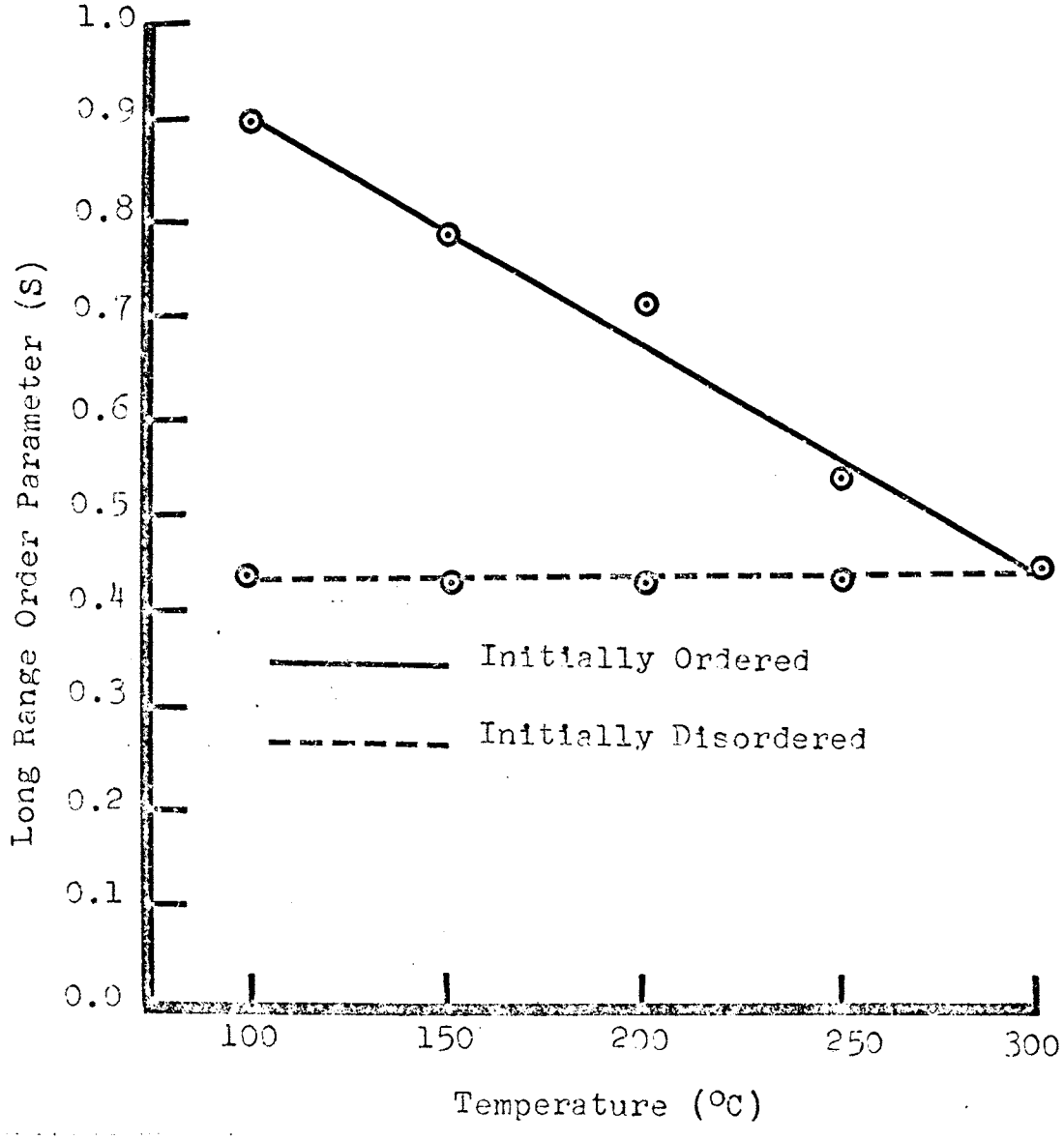

Figure 16. The Change in Order Parameter at Various Temperatures of Irradiation. Total Dose 19.2×10^{13} n/cm^2 as Determined by Toma(24).

CHAPTER III

EXPERIMENTAL PROCEDURE

A. Specimen Preparation:

The alloy used in this investigation was obtained from the Naval Ordnance Laboratory in sheet form of approximately 0.038 inches thick. The composition as determined by them was as follows:

Aluminum	13.79 weight per cent (w/o)
Carbon	0.0045 w/o
Sulfur	0.0020 w/o
Hydrogen, Oxygen and Nitrogen	less than 0.0001 w/o
Iron	Remainder

This composition is as close as reasonably possible to stoichiometric Fe_3Al.

The material was sheared from the sheet into strips approximately 3/4 of an inch wide by 12 inches long. The edges of these strips were ground to relieve as much of the disturbed metal resulting from the shearing as possible. All specimens were prepared in this manner to assure uniformity of specimens. The final dimensions of the specimens were 1/2 inches by 0.038 inches thick.

The first specimen was heated to 800°C and held for 3 hours and then cooled to room temperature at a cooling rate of 25°C/hour. Specimen number two was heated to 800°C, held for 3 hours, cooled at a rate of 25°C/hour down to 200°C and then quenched in water. Specimen number three was heated to 800°C, cooled at a rate of 25°C/hour down to

room temperature, reheated to 400°C and held for 2 1/2 hours and the water quenched. Specimen number four was heated from the as received condition up to 500°C and held for 3 hours and then water quenched. The last specimen, specimen number five was heated up to 800°C and held for 3 hours and then water quenched. These five heat treatments gave state of order ranging from completely ordered to completely disordered and various intermediate states.

After these specimens were heat treated every effort was made to assure minimum of handling so as to avoid introducing defects. The next step in the specimen preparation was to spotweld 4 copper electrical leads to each specimen. The distance between the middle two was approximately 8 inches. The distance between the outer two was of little concern, but was somewhere near 9 inches. The distance between inner lead was measured very precisely with a pair of calipers and used as the gauge length for calculating the total resistivity. A specimen with electrical leads attached is shown in Figure 17.

B. Encapsulation:

Since it was desirable to keep the specimen from direct contact with the coolant/moderator, a cylindrical capsule was devised to accomodate the specimen. This capsule was constructed entirely of commercially pure aluminum to reduce residual radiation and also to cut down on the absorption of thermal neutrons while in the core.

The capsule was 3 inches in outside diameter and 2 1/2

Figure 17. Typical Specimen With Electrical Leads Spot-Welded In Place.

inches inside diameter. Total length of capsule was approxi - mately 24 inches. Both ends were fitted with aluminum plugs which were fitted with "O" rings and held in position by horizontal drift pins.

A 3/4 inch diameter thin walled aluminum tube was attached by welding to the top plug and a hole drilled in the top plug thereby giving a means of access to the capsule. The tube itself was approximately 35 feet long with a curved section about 10 feet above the capsule to eliminate gamma ray streaming up the tube.

A specimen holder was fabricated out of 1/4" plexi - glass which comprised two discs held together by long aluminum rods threaded at both ends. A slot was made in the opposing faces of the plexiglass discs into which the specimen was placed and held by adjusting the tension on the aluminum rods. Holes for lead wires and coolant flow were also drilled in the top plexiglass disc. A cross sectional view of the capsule with specimen, specimen holder and attached accessories is shown in Figure 18.

The capsule with specimen removed and laying along side can be seen in Figure 19. A radiation detector is also shown next to the specimen indicating a safe level of radiation after a cooling off period of two days had elapsed since irradiation.

The cooling tube that is seen in Figure 18 was used to flow nitrogen at a slow rate to cool the capsule and specimen that had undergone gamma ray heating during 12 hours of irradiation. The flow rate was approximately 4

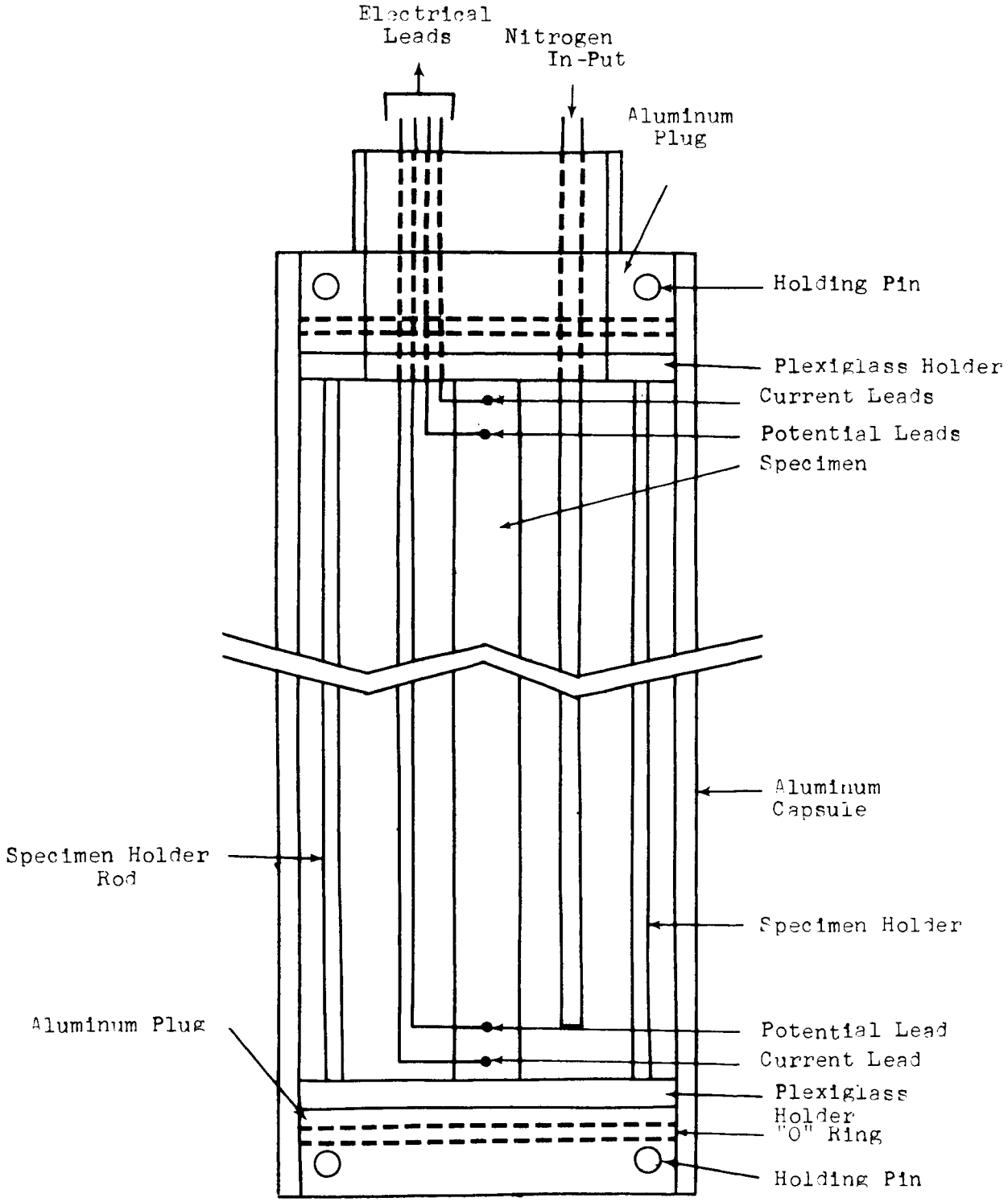

Figure 18. Cross Sectional View of Capsule and Specimen.

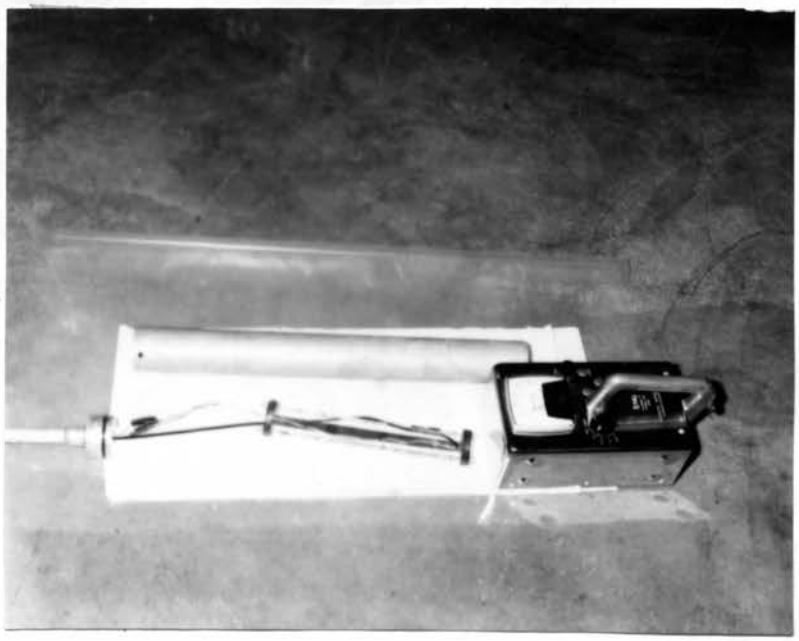

Figure 19. Actual Specimen and Holder Removed From Capsule After Irradiation.

cubic feet per hour.

C. Resistivity Measurements:

The four electrical leads attached to each specimen were conveyed from the capsule through the tube to a double precision Kelvin bridge and supporting equipment at the side of the reactor pool.

A dry cell supplied a 6 volt potential across the specimen and by means of a variable resistor a current of 1 amp was obtained for the total system. The two inside leads picked-up the potential drop across the gauge length and balanced it against a standard resistor of 0.001 ohm by means of the Kelvin bridge. The resistance of the specimen across the gauge length was then read directly from the Kelvin bridge. A schematic diagram of the electrical circuit of the specimen and Kelvin bridge is shown in Figure 20. An actual photograph of the experimental setup is shown in Figure 21.

The resistivity is then calculated by multiplying the resistance by the cross sectional area of the specimen and then dividing that by the gauge length or the distance between inside electrical leads. During the actual experiment only the resistance was recorded versus the time of irradiation. Later the resistance was converted to resistivity and the time of irradiation to dose.

Figure 22 shows the complete out-of-the-core apparatus used in the experiment. Also visible to this figure is the side of the reactor pool and the bridge superstructure from which the reactor core is suspended.

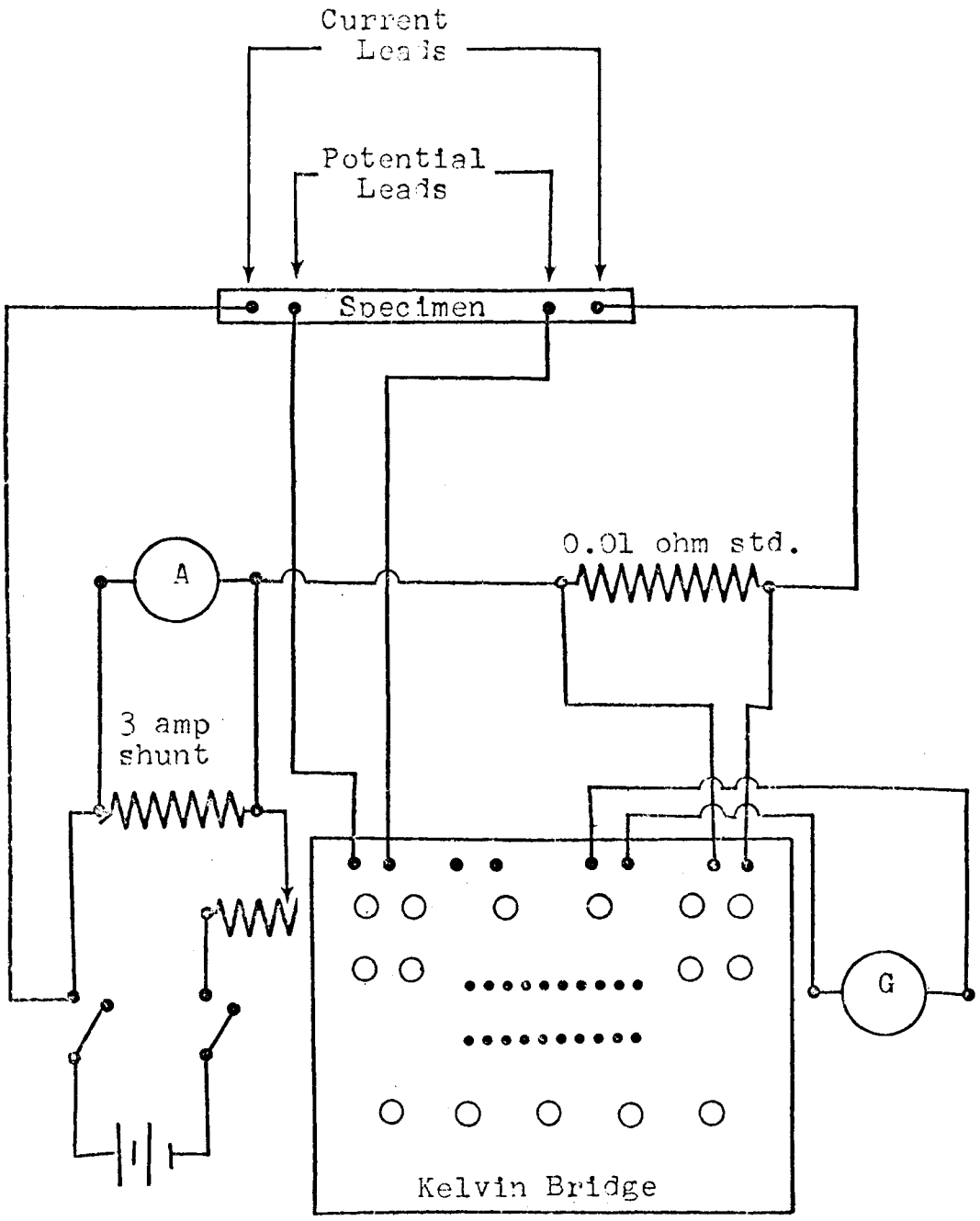

Figure 20. Schematic Diagram for Resistivity Measurements.

Figure 21. Actual Physical Set-Up For Resistivity Measurements.

Figure 22. Physical Set-Up Showing Kelvin Bridge and Nitrogen Supply.

D. The Reactor.

The reactor used for this investigation was a swimming pool modified Bulk Shielding Reactor type with a maximum thermal output of 10 kilowatts. During the entire investigation the reactor was operated at a power level of 10 kilowatts which produced a fast neutron flux of 3.4×10^9 neutrons/cm^2-sec. at position C-3, the core configuration used was the 19-T core loading and core position C-3 was used in all cases. Each experiment was conducted for approximately 12 to 16 hours depending upon staff member availability. The temperature in the reactor bay area ranged between 25°C to 32°C during the tests. Specimen temperature was in the range of 30 to 40°C.

CHAPTER IV

EXPERIMENTAL RESULTS

A. Resistivity

As mentioned previously the resistance of the specimen was measured as a function of time and then converted to resistivity and the time converted to dose. The results of these experiments are shown in Figure 23, 24, 25, 26 and 27.

Figure 23 is the resistivity versus the dose curve for the fully ordered specimen number 1 and shows the lowest resistivity of all specimens irradiated. The rate of damage appears to be constant. Later experiments will show it to be greatest in the first few hours, then becomes almost constant as the dose increases.

Figure 24 is the resistivity versus the dose curve for the slightly disordered specimen number 2. Here the rate of irradiation damage is very high for the first hour or more and then decreases to a slower rate and finally almost goes to zero as the dose (time) increases.

Figure 25 is the resistivity versus the dose curve for specimen number 3 which is a little more disordered than the preceeding specimen. Again the damage rate was greatest during the first few hours. In this case, however, the damage rate does not drop off to zero but continues to increase as dose increases.

Figure 26 is the resistivity versus the dose curve for specimen number 4 which is only slightly ordered. Here the

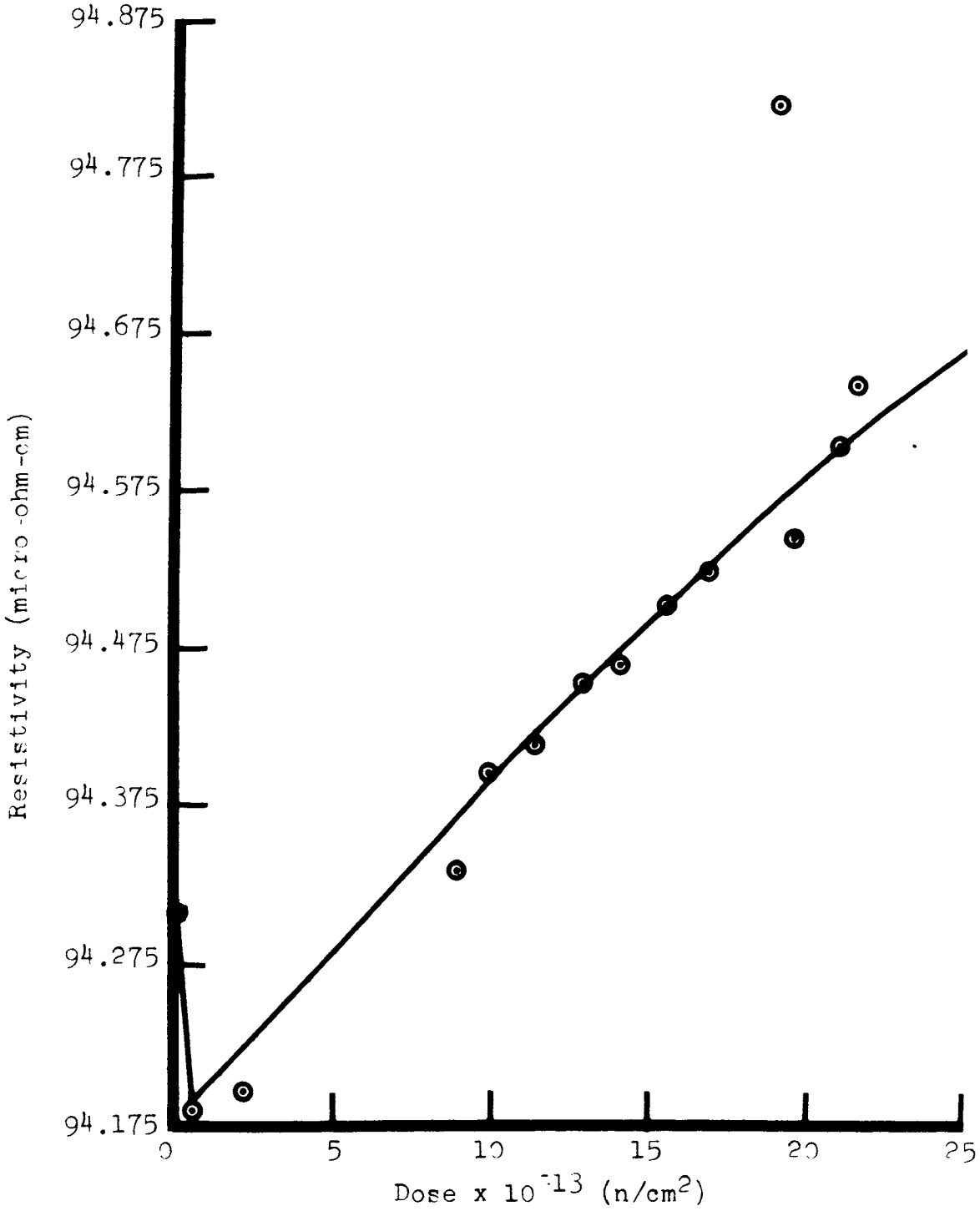

Figure 23. Resistivity vs. Dose For Ordered Fe_3Al.

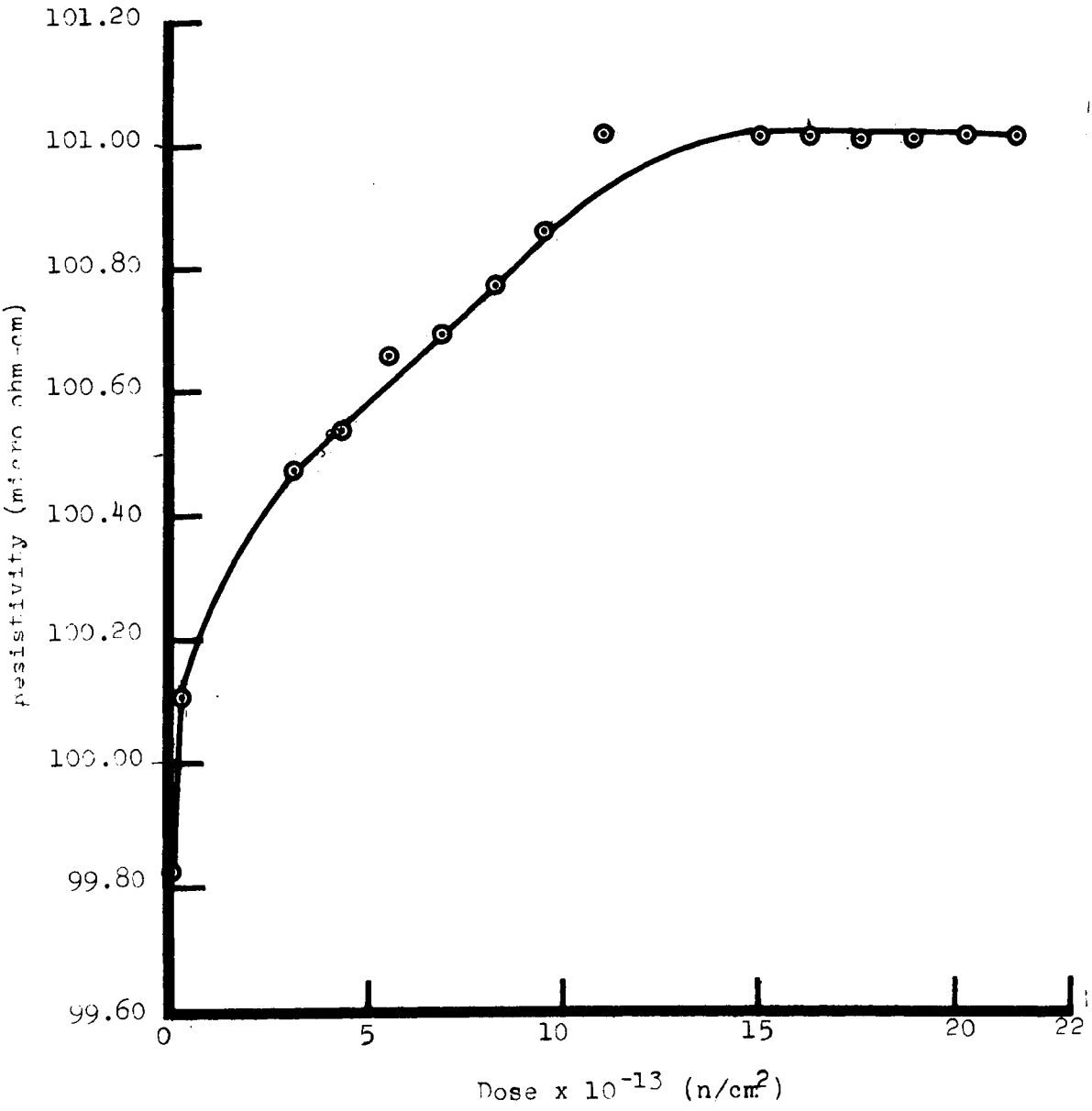

Figure 24. Resistivity vs. Dose For Partially Disordered Fe_3Al.

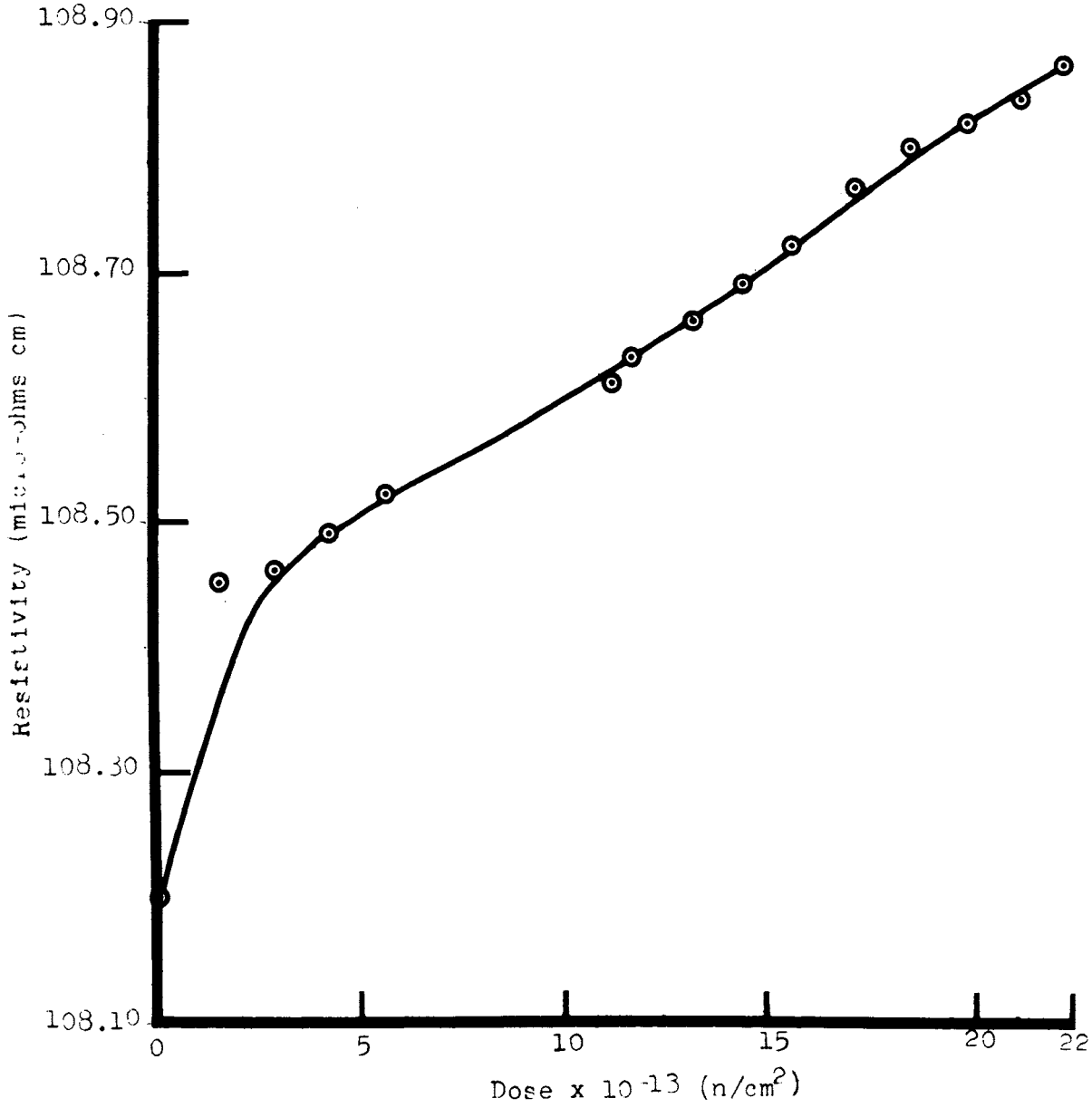

Figure 25. Resistivity vs. Dose for Partially Disordered Fe_3Al.

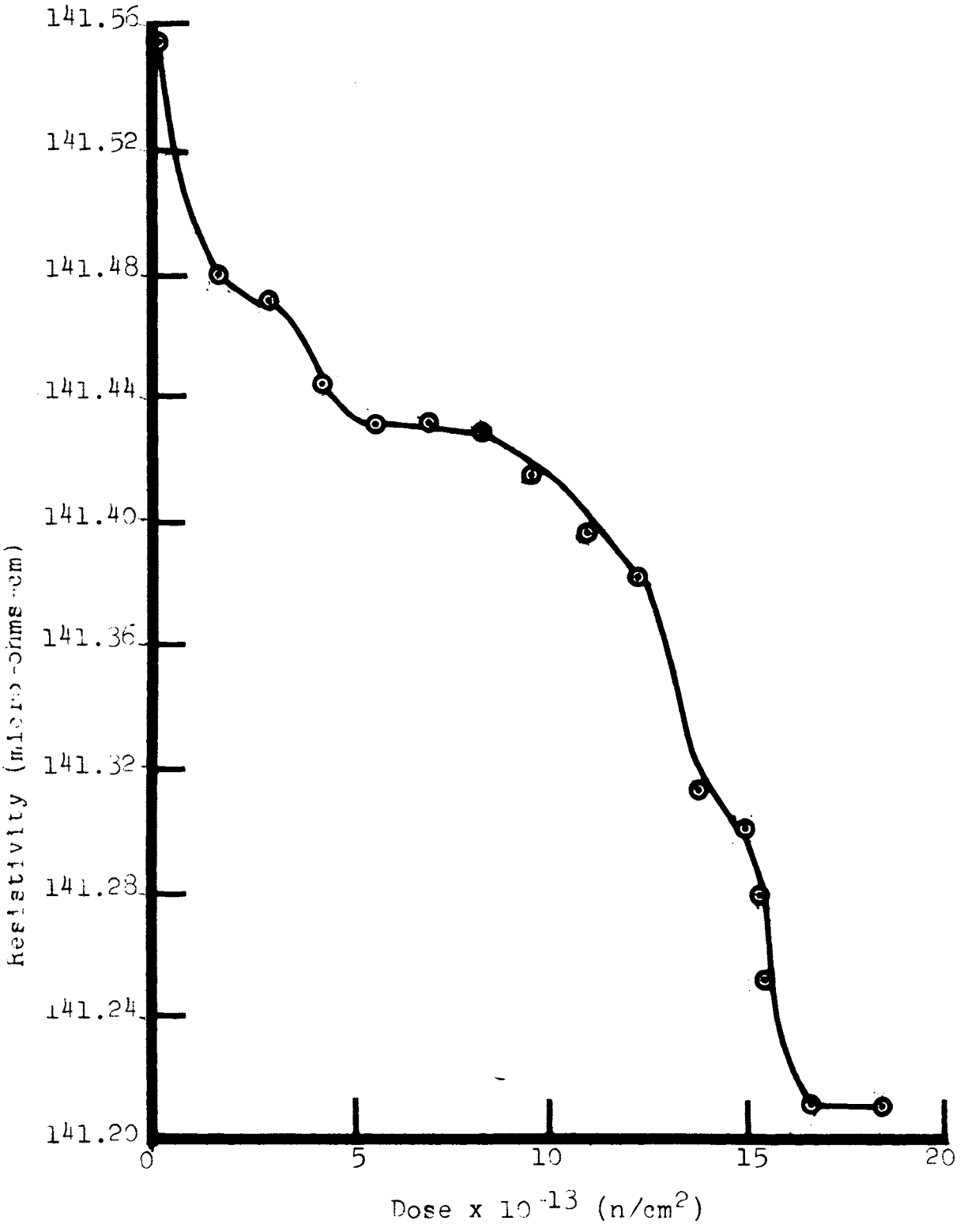

Figure 26. Resistivity vs. Dose For Partially Ordered Fe_3Al.

plateaus are very evident and there appears to be approximately 3 of them. Again the resistivity decreases as the dose increases. This decrease in resistivity with increasing dose indicates an increase in order in the specimens. In the ordered specimens there is a tendency for the alloy to increase in resistivity with increasing dose therefore causing a decrease in order.

Figure 27 is the resistivity versus dose curve for the fully disordered alloy specimen number five. The resistivity for this specimen is the highest of all as should be expected, (143.697 micro-ohm cm). There appears to be plateaus at two different levels in the graph where the dose rate seems to approach a low value, not zero but considerably less than the remainder of the curve. Here a definite decrease in resistivity is apparent as dose increases, whereas in the ordered specimens there was a definite tendency to increase resistivity with increased dose.

B. Order Parameters:

Figures 28-32 show the change in the order parameter S, as calculated from the Muto's relationship, (see equation 5), as a function of dose for the five specimens. The general shapes of the curves are the inverse of their respective resistivity curves as should be expected. The long range order parameter S is calculated using 94.178 micro-ohm-cms as the resistivity of the fully ordered state and 143.697 micro-ohm-cms as the resistivity of the full disordered state. These graphs are given here mainly

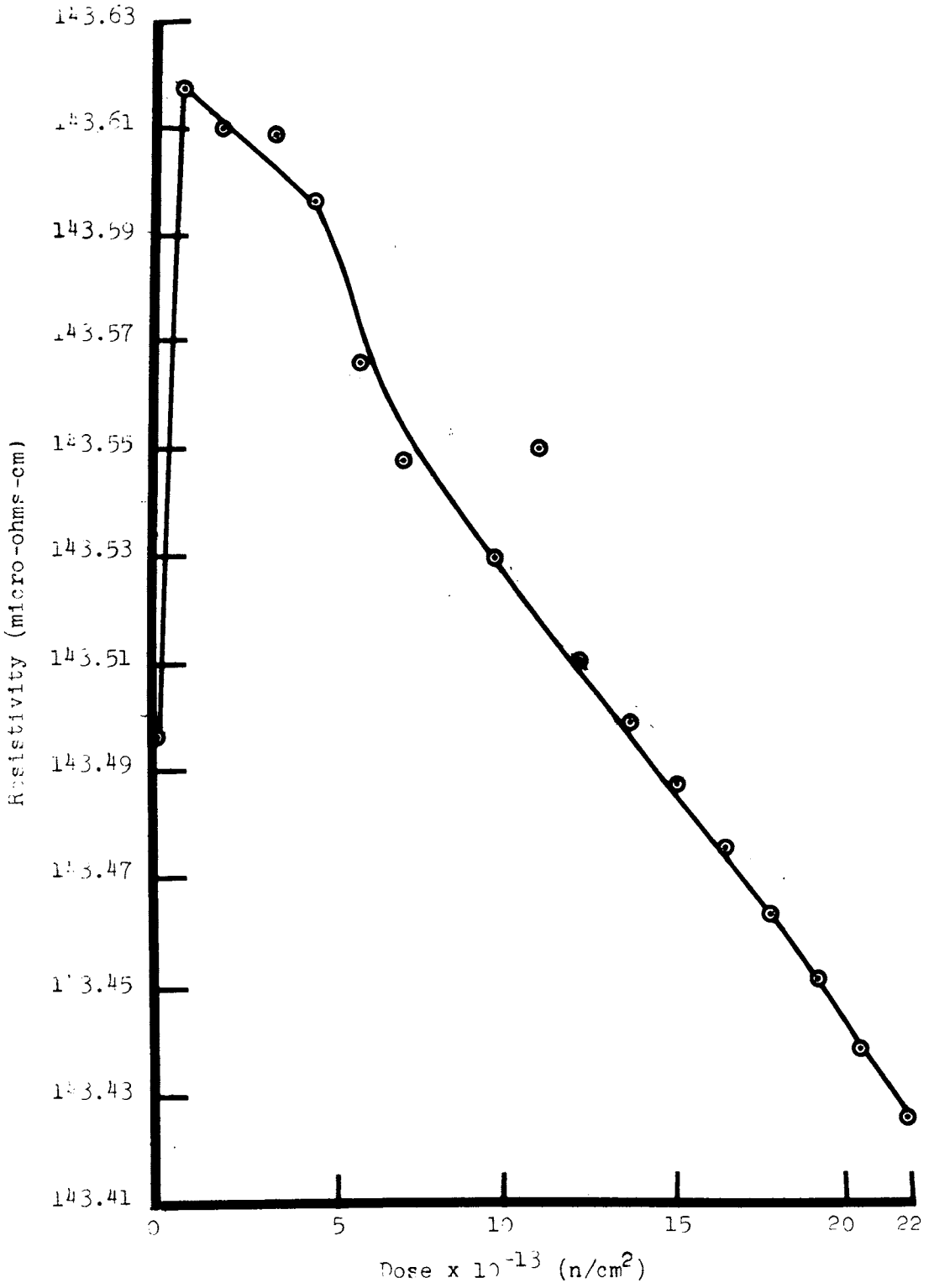

Figure 27. Resistivity vs. Dose For Disordered Fe_3Al.

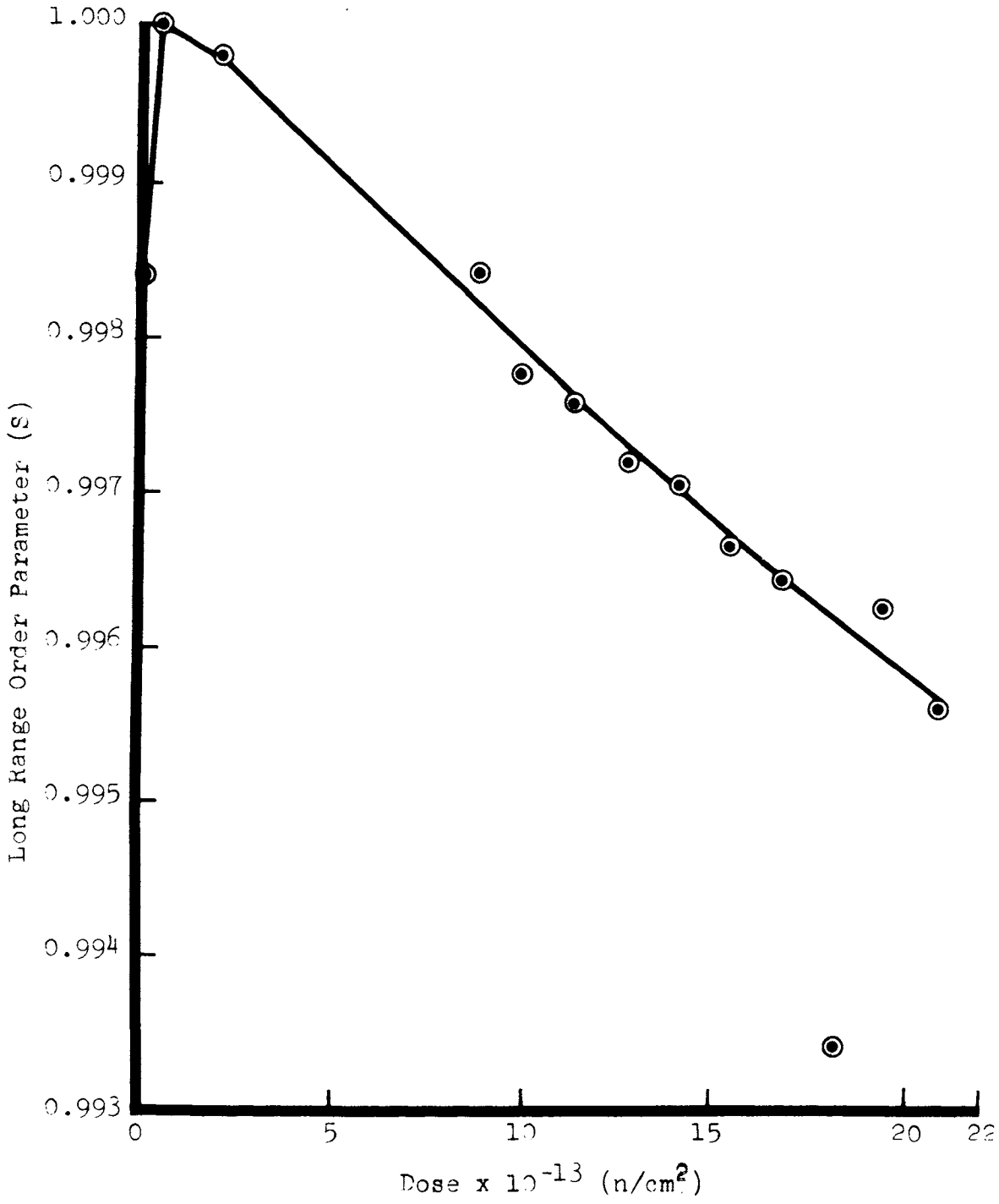

Figure 28. Long Range Order Parameter (S) vs. Dose For Ordered Fe_3Al.

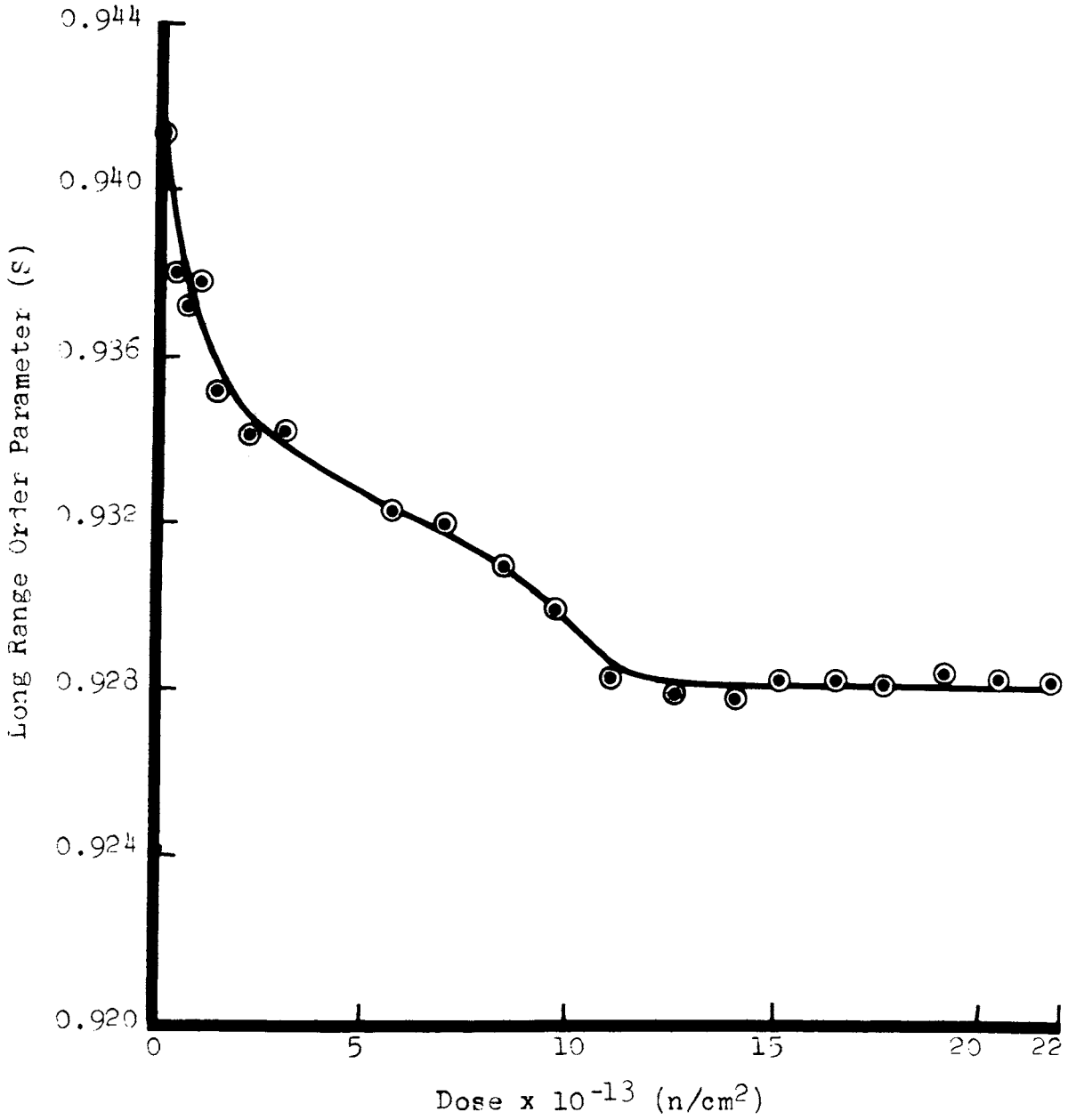

Figure 29. Long Range Order Parameter (S) vs. Dose For Partially Disordered Fe_3Al.

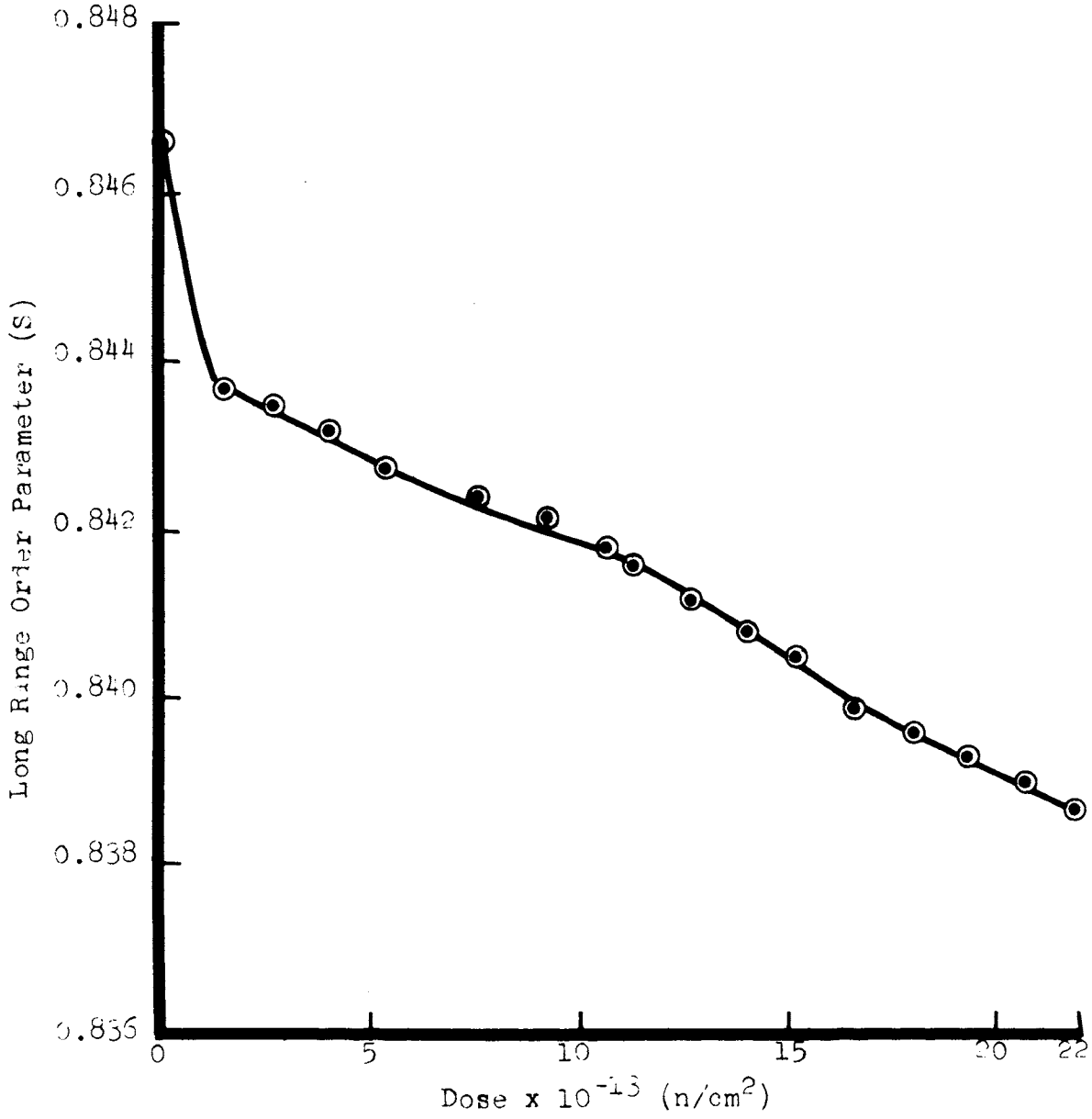

Figure 30. Long Range Order Parameter (S) vs. Dose For Partially Disordered Fe_3Al.

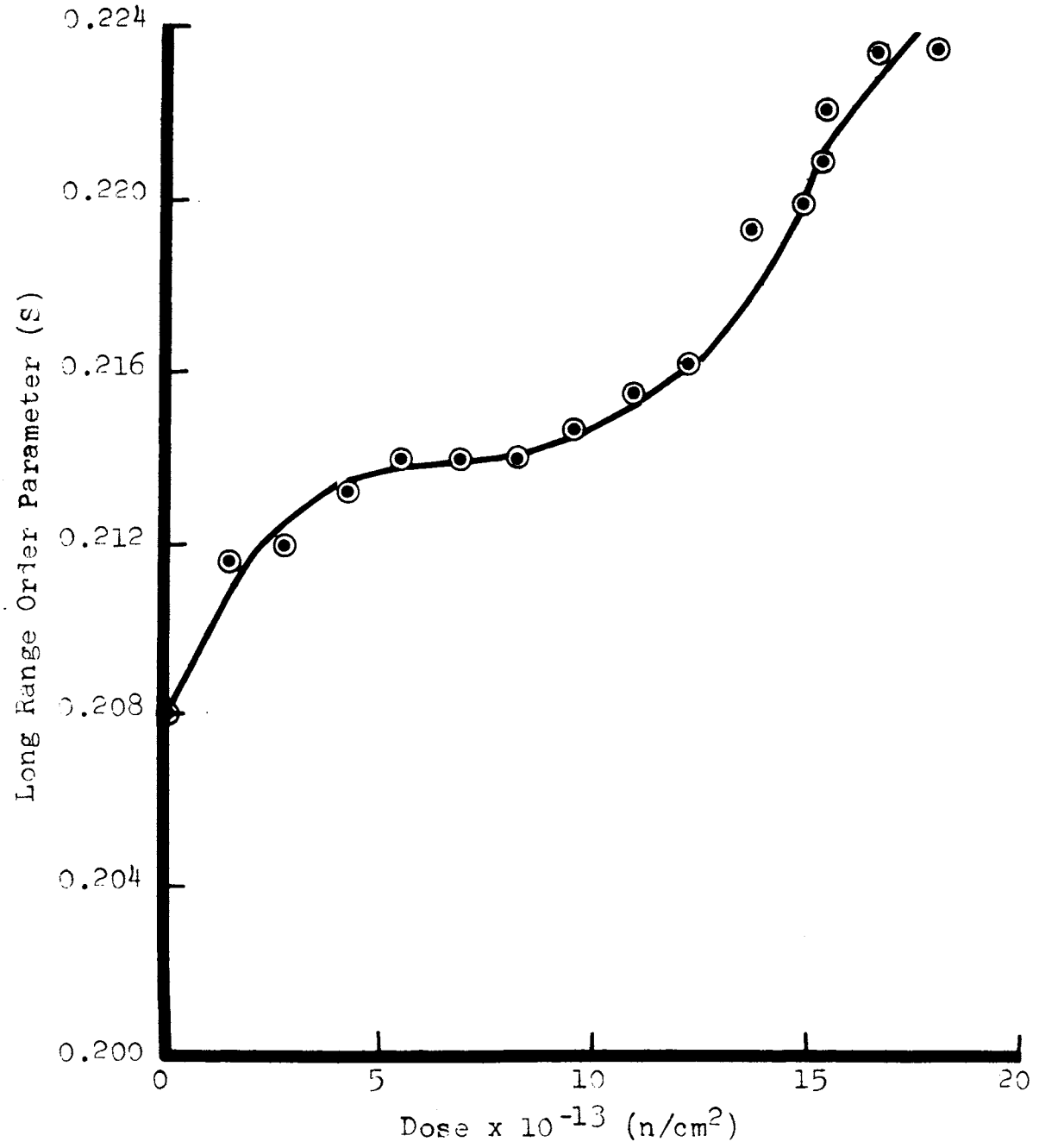

Figure 31. Long Range Order Parameter (S) vs. Dose For Partially Ordered Fe_3Al.

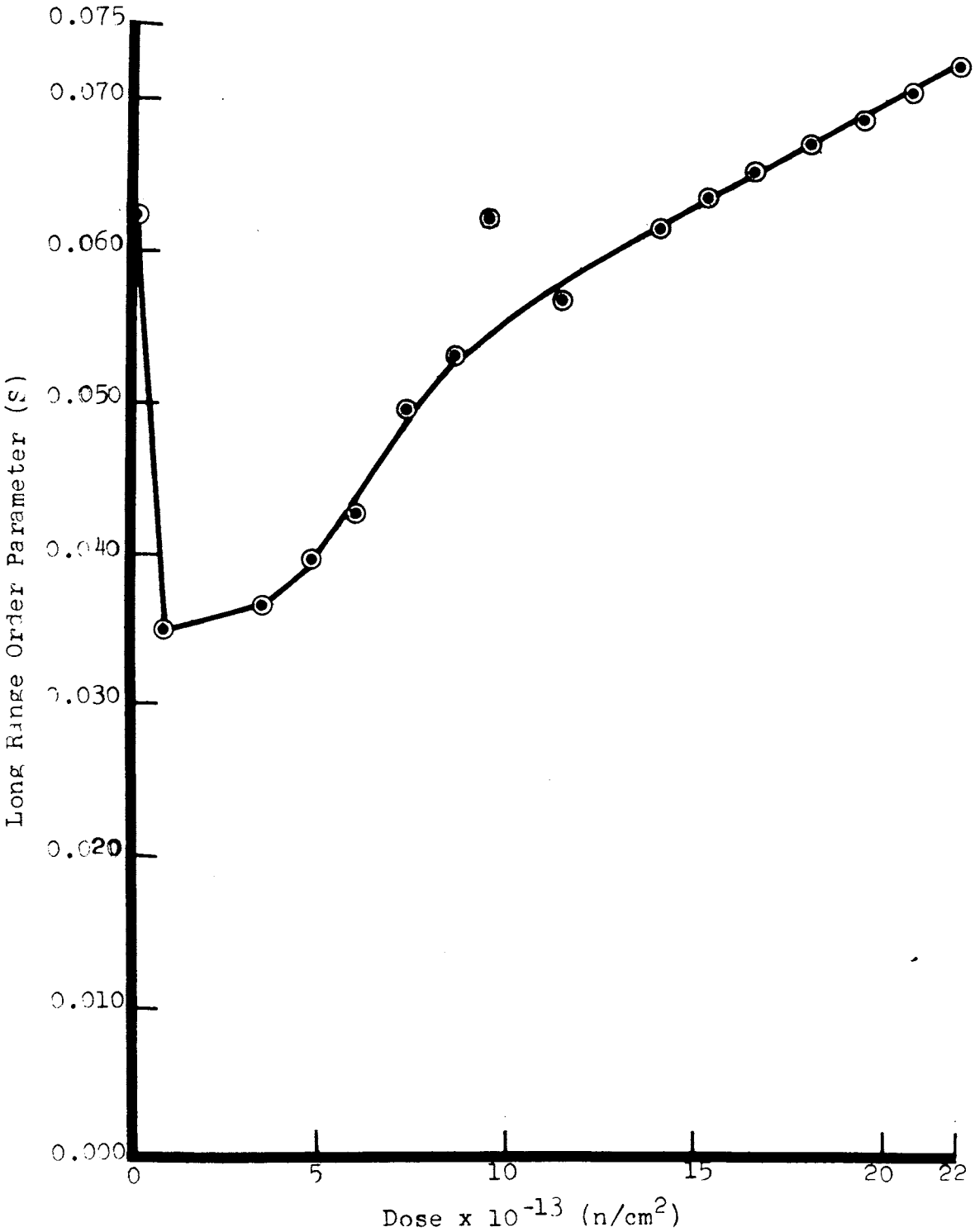

Figure 32. Long Range Order Parameter (S) vs. Dose For Disordered Fe_3Al.

TABLE III

Irradiation Damage Rates

Specimen No.	Initial Order Parameter(S)	Damage Rates in $\frac{\text{micro-ohm-cm}}{\text{neutrons/cm}^2}$	
		Initial	Equilibrium
1 (ordered)	1.00	18.7×10^{-15}	1.93×10^{-15}
2	0.94	79.2×10^{-15}	0.537×10^{-15}
3	0.84	16.6×10^{-15}	2.06×10^{-15}
4	0.20	16.5×10^{-15}	4.05×10^{-15}
5 (disordered)	0.00	5.28×10^{-15}	0.902×10^{-15}

to simplify the visual picture of what takes place in the atomic arrangement during irradiation. They show that order decreases with increasing irradiation of fully ordered and slightly-disordered specimens whereas, the disorder decreases with increasing irradiation for fully disordered and slightly ordered states.

C. Damage Rates:

The initial and "equilibrium" rates of damage were calculated for the five specimens and are tabulated in Table III. The initial period was considered the first hour after start-up of the reactor and was determined from the first two data points on each graph of resistivity versus dose. The "equilibrium" damage rate was taken over the latter portion of each curve and is termed equilibrium only because it is supposed that all factors influencing the damage rate have reached equilibrium. This might also be called a psuedo-equilibrium because in some cases the slopes or damage rates are actually decreasing with increasing doses but they are approaching equilibrium status. The damage rate is measured in units of micro-ohms-cm/neutron/cm^2 or resistivity/dose.

CHAPTER V

DISCUSSION OF RESULTS

A comparison of Saenko's[34] and Toma's[24] results with the results found in this investigation show considerable similarities. Saenko's results can be found in Figure 15 and Toma's in Figure 16. Comparing these two investigations with those of the author show the same tendency for the ordered specimens to become more disordered with increasing radiation dose and the disordered specimens tend to become more ordered.

Neither Saenko or Toma show the initial increase in order for the ordered specimen nor the initial decrease in order of the disordered specimen during the first hour of irradiation as was observed in this research. The possible reason this is not found in Saenko's work is the high fast neutron flux used in his work (approximately 5×10^{14} neutrons/cm^2 sec.) as compared to the fast neutron flux used in this investigation (3.4×10^9 neutron/cm^2 sec). In Toma's work it is not seen because of the elevated temperatures used, since, as will be discussed later, this is a temperature and equilibrium dependent phenomena.

Saenko and Toma both determined an equilibrium time or dose such that the order parameter or resistivity remained somewhat constant with increased dose. This point was not reached in this investigation as the long time or dose necessary for this to occur was not possible under the present reactor operating conditions.

By extrapolation of the data of this investigation the resistivity at this equilibrium point appears to be approximately 130-135 micro-ohms-cm. which should be reached at an estimated dose of 1.02 x 10^{20} neutrons/cm^2. Saenko's results show it to be at approximately 138 micro-ohms cm. and a total dose of about 1.20 x 10^{20} neutrons/cm^2. Toma showed this point to be at 142 micro-ohms cm at a total dose of 1.92 x 10^{14} neutrons/cm^2 but at an elevated temperature of 300°C. These results are in good agreement since a higher resistivity should be expected for a specimen that is at the higher temperature and after a shorter dose.

A. Resistivity Changes:

Looking closer at the initial change in the resistivity shows in the case of the ordered specimen, Figure 23, a decrease in resistivity initially then an upswing in resistivity, indicating a more disordered state is forming. This initial decrease in resistivity of the ordered specimen was also found by Cook and Cushing[27] and Adams et al.[36] in their investigation of the copper-gold alloy Cu_3Au. They attributed this change largely to thermal neutron effects of transmutation of the gold atom. In the alloy under consideration in this investigation it is more than likely that the iron atom would be the atom undergoing the transmutation that turns the system from a two element ordered alloy to a three element ordered alloy. However, for this to occur Fe^{58}, whose abundance is only 0.31%, would have to capture a neutron (cross section = 1.2 barns) to form Fe^{59}

which would decay to Co^{59} by β emmission. The half life of Fe^{59} is 45 days thereby making transmutation highly unlikely for the drop in resistivity seen in this alloy.

Temperature also has an effect on the resistivity of the alloy under investigation. Cook and Cushing[27] point out that during the time of initial start-up of the reactor and the time the first measurement is made the specimen has encountered a temperature rise in the surroundings and its temperature has increased due to gamma ray heating and the heat given off by the nuclear process occurring in the reactor core. This increase in temperature causes some of the atoms that were disordered due to handling of the specimen or as in this investigation disordering due to spotwelding the electrical leads to the specimen to become ordered. Cook and Cushing also suggest that the best order state obtainable by slow cooling is that found at 200°C and the temperature rise occured in reactor start up anneals out some of the disordered phase found in the specimen.

Kinchin and Pease[37] found this initial decrease in resistivity of an ordered specimen of Cu_3Au during irradiation. However, in their work they contend that it is due strictly to a temperature effect as mentioned previously and not to any transmutation. Kinchin and Pease claim that at room temperature the times necessary to reach equilibrium are so long all the ordered alloys have appreciably less than the equilibrium of order. Therefore upon irradiation with fast neutrons, vacancies are produced within the lattice and vacancies have been found to increase the rate

of ordering so thereby causing the ordered alloy to approach the true equilibrium state for room temperature. This process occurs until such time as the number of vacancies, interstitials and other disordering mechanisms override the ordering rate created by the vacancies. Therefore not only is the order state of the alloy temperature sensitive but its ordering rate is vacancy sensitive. It would appear that this vacancy sensitivity has a greater initial effect on the decrease of the resistivity of the ordered specimen than does the increase in temperature during start-up.

Temperature sensitivity of the specimens resistivity was also noted during irradiation when the nitrogen flow was halted due to the nitrogen tank running dry. This can be seen by the point on Figures 28 and 32 which is completely out of proportion with the rest of the points. In both cases when the nitrogen supply ran out the resistivity increased due to a temperature rise. This temperature rise was approximately 10-15°C as determined by the resistivity change.

In the quenched disordered specimen, Figure 27, an increase in resistivity during the initial hour was noted. Since the number of vacancies is already sufficient for any ordering rate increase to be near maximum for that specimen then the increase in disorder must be caused by the increase in temperature. This increase in temperature is of the order of 40-50°C and is due largely to gamma ray heating and the increase in the core and coolant temperature brought on by the nuclear fission process. This increase in

resistivity is calculated to be 0.133 micro-ohms-cm and by using Toma's[24] and Rauscher's[18] data an increase in temperature of the order of 40-50°C should bring about an increase in resistivity of approximately 0.150 micro-ohms-cm which is within agreement with the change in resistivity found here. It is therefore postulated that the increase in resistivity in the disordered specimen is due to a temperature increase and the resistivity decrease in the ordered specimen is due to vacancy introduction which increases the ordering rate and an increase in temperature which anneals out the localized disordered domains. In the disordered specimen the disorder is of such a high degree that the temperature increase acts only to increase the resistivity whereas in the ordered specimen the ordering is very near to the perfect state that the temperature increase acts to further order the specimen.

After the initial period of 1 to 1 1/2 hours had passed, the specimens behaved much as expected, i.e., the disordered specimens tended toward a more ordered state and the ordered specimen toward a more disordered state. The only variation seen was in specimen 4 which shows up in Figure 26 as plateaus. These plateaus are probably due to a similar effect of domain ordering as found by Seybolt.[35] The disordered state in the 510°C was found by Seybolt to order by slope changes as the temperature was lowered. This ordering he claimed was accomplished by the ordering of small domains which grow effecting the overall resistivity only slightly until a critical volume is reached which decreases the

resistivity. This can be thought of as the formation of short range order domains in a totally disordered specimen.

These plateaus are possibly due also to a combination of ordering mechanisms. That is, the rate of ordering for a given state of disorder can be controlled by a different mechanism then a slightly higher degree of disorder thereby an increase in order would change the order rate and therefore change the slope of the curve of resistivity versus dose. This same sort of mechanism change has been postulated in the activation energy studies[24,38] of this alloy.

B. Long Range order Parameter Changes:

The change in the long range order parameter S with increasing dose is shown in Figures 28-32 in descending order of their initial order parameter value. The graphs are shown here for simplification of viewing and ease of understanding. Since in these graphs the higher the order the higher the order parameter S, it is easier to see a decrease in disorder because it occurs as a decrease in the curve. The graphs follow the same pattern as found in the resistivity versus dose graphs except in the reverse fashion. The initial change in order is noted in Figure 28 and 32 as was seen in Figures 23 and 27 and merit no further discussion.

C. Damage Rates:

The damage rates calculated show a very definite change between the initial and the equilibrium rate. The initial rate is considerably greater than the equilibrium rate as is readily noticeably from Table III or from Figures 23-27. The reason behind this greater damage rate at the onset of

irradiation is the influencing role of the temperature rise. The temperature increase is adding to the change in resistivity which increases the damage rate but cannot actually be considered as irradiation damage. The fast neutrons are colliding with the atoms causing displacement and thereby creating the total damage as recorded in Table III.

As time passes the temperature effect decreases and reaches an equilibrium state thereby contributing very little to the damage rate. At this point the equilibrium damage rate is calculated and more nearly represents the damage rate for fast neutrons. The damage rate for fast neutrons being considerably less than the initial damage rate.

The extremely high initial damage rate for specimen number two is not readily understood but may be due to an unusually large temperature increase incurred during start-up and the first hour of running. Since the equilibrium damage rate for this specimen is in line with those of the other specimens, it would then appear that only the initial damage rate is in question. By taking the second and third points on the graph of specimen number 2 (Figure 24) for calculating the initial damage rate a value of 12.48×10^{-15} $\frac{\text{micro-ohms-cm}}{\text{neutrons/cm}^2}$ is derived. This value is more in line with the other values thereby leading one to believe something unexplainable occured during the first hour of irradiation.

The low initial damage rate of specimen number five (Figure 27) is carried through into the equilibrium damage

rate as seen in Table III. Other investigators (26,27,30, 34 and 36) have also recorded lower damage rates for the completely disordered state as compared to the ordered state. This is easily explained by the fact that the probability of disordering a completely ordered state is greater than ordering a completely disordered state. The damage rate for fast neutrons according to this data is in the range of 0.5 - 5.0 x 10^{-15} $\frac{\text{micro-ohms-cm}}{\text{neutrons/cm}^2}$ and the combined damage rate attributed to temperature and other effects is initially approximately 10 x 10^{-15} $\frac{\text{micro-ohms-cm}}{\text{neutrons/cm}^2}$.

CHAPTER VI

CONCLUSION

The resistivity measurements determined in this investigation show a definite tendency for ordered specimens to become disordered and disordered specimens to become ordered with increased time of irradiation in a reactor.

The temperature effect is very noted during initial 1 to 1 1/2 hours after reactor start-up. The findings of Kinchin and Pease[37] are further enhanced over those of Cook and Cushing[27] as to the temperature and not thermal neutrons causing the initial drop or rise in resistivity during start-up and first hour of irradiation.

Equilibrium damage rates were found to be in the range of 0.5 to 5.0 x 10^{-15} $\frac{\text{micro-ohms-cm}}{\text{neutrons/cm}^2}$ whereas initial damage rates were of the order 5.0 to 20 $\frac{\text{micro-ohms-cm}}{\text{neutrons/cm}^2}$.

CHAPTER VII

RECOMMENDATIONS

Since the effects of irradiation can anneal out at relatively low temperature it is suggested that a series of experiments be run using liquid nitrogen or helium temperatures during irradiation to "trap" the larger part of the defect in the crystal.

It is also suggested that a study of irradiated specimens be made using the electron microscope to detect any large areas of radiation damage occuring in the specimens. Also a Mossbauer effect experiment might be run on the samples since they contain iron.

APPENDIX

APPENDIX A

Experimental Data

Specimen No. 1

Ordered Fe_3Al Reactor Power: 10 KW

Gauge Length: 8.28125 in. Width: 0.5343 in.

Thickness: 0.0395 in.

Resistance (μ ohms)	Resistivity (μ ohms-cm)	Dose x 10^{-13} (n/cm^2)
145.63	94.307	0.000
145.43	94.178	0.689
145.46	94.197	2.137
145.67	94.333	8.867
145.77	94.398	9.970
145.80	94.417	11.438
145.86	94.456	12.811
145.88	94.469	14.127
145.94	94.508	15.461
145.97	94.527	16.794
146.43	94.825	18.087
146.00	94.547	19.425
146.10	94.611	20.828
146.15	94.644	21.516

Specimen No. 2

Partially Disordered Fe_3Al Reactor Power: 10 KW

Gauge Length: 7.906 in. Width: 0.5615 in.

Thickness: 0.0395 in.

Resistance(μohms)	Resistivity(μohms-cm)	Dose x 10^{-13}(n/cm^2)
140.03	99.816	0.000
140.34	100.137	0.405
140.96	100.479	3.148
141.05	100.543	4.401
141.21	100.657	5.687
141.26	100.693	7.034
141.38	100.778	8.346
141.50	100.864	9.678
141.72	101.021	11.076
141.72	101.021	15.136
141.72	101.021	16.379
141.74	101.035	17.744
141.70	101.010	19.100
141.72	101.021	20.401
141.72	101.021	21.707

Specimen No. 3

Partially Disordered Fe_3Al Reactor Power: 10 KW

Gauge Length: 8.1875 in. Width: 0.5585 in.

Thickness: 0.0365 in.

Resistance (μohms)	Resistivity (μohms-cm)	Dose x 10^{-13} (n/cm^2)
171.03	108.204	0.000
171.42	108.451	1.487
171.44	108.463	2.743
171.48	108.484	4.064
171.54	108.526	5.397
171.67	108.609	10.793
171.70	108.628	11.274
171.75	108.659	12.673
171.80	108.691	13.967
171.84	108.716	15.259
171.92	108.767	16.636
171.96	108.792	18.014
172.00	108.816	19.327
172.04	108.843	20.667
172.08	108.868	21.945

Specimen No. 4

Partially Ordered Fe_3Al Reactor Power: 10 KW

Gauge Length: 8.1562 in. Width: 0.5628 in.

Thickness: 0.0391 in.

Resistance(μohms)	Resistivity(μohms-cm)	Dose x 10^{-13}(n/cm^2)
206.48	141.554	0.093
206.37	141.479	1.513
206.36	141.472	2.813
206.32	141.445	4.129
206.30	141.431	5.523
206.30	141.431	6.935
206.30	141.431	8.188
206.28	141.417	9.503
206.25	141.397	10.899
206.23	141.383	12.193
206.13	141.314	13.750
206.11	141.301	14.887
206.08	141.280	15.281
206.04	141.253	15.404
206.00	141.225	16.628
206.00	141.225	18.041

Specimen No. 5

Disordered Fe_3Al Reactor Power: 10 KW

Gauge Length: 8.7187 in. Width: 0.5610 in.

Thickness: 0.0370 in.

Resistance(μohms)	Resistivity(μohms-cm)	Dose x 10^{-13}(n/cm^2)
237.22	143.504	0.091
237.44	143.637	0.897
237.43	143.631	3.525
237.41	143.619	4.683
237.39	143.607	5.973
237.34	143.576	7.339
237.31	143.558	8.606
237.27	143.534	10.011
237.31	143.558	11.334
237.25	143.583	12.687
237.23	143.510	14.006
237.21	143.498	15.374
237.19	143.486	16.694
237.17	143.474	18.064
237.15	143.462	19.381
237.13	143.449	20.689
237.11	143.437	22.012

BIBLIOGRAPHY

1. BRADLEY, A. J. and A. H. JAY (1932) Journal of the Iron and Steel Institute, 125, p. 339.

2. GUY, A. G. Elements of Physical Metallurgy, Addison-Wesley Publishing Co., Inc., 2nd Edition, p. 73.

3. AVNER, S. H. Introduction to Physical Metallurgy, Mc Graw-Hill Book Co., Inc., p. 61.

4. CULLITY, B. D., Elements of X-Ray Diffraction, Addison-Wesley Publishing Co., Inc. Second Printing, p. 29.

5. REED-HILL, R. E., Physical Metallurgy Principals, D. Van Nostrand Co., Inc., p. 343.

6. NIX F. and SHOCKLEY W. (1938) Rev. of Modern Physics, 10, p. 1.

7. BARRETT, C. S., Structure of Metals, McGraw-Hill Book Co., Inc.

8. MUTO, T. and TAKAGI, Y. (1956), The Theory of Order-Disorder Transistions in Alloys, Solid State Physics Reprints, Academic Press.

9. BRAGG, W. L. and WILLIAMS, E. J. (1934), Proceedings of the Royal Society, Vol. A 145, p. 699.

10. BETHE, W. (1935), Proceedings of the Royal Society, Vol. A150, p. 522.

11. HANSEN, M. and ANDERKO, K. (1958) Constitution of Binany Alloys, McGraw Hill, New York.

12. TAYLOR, A. and JONES, R. (1958) Journal of Physics and Chemistry of Solids, Vol. 6, p. 16.

13. McQUEEN, H. and KUCZYNSKI, G. (1959) Transactions of the A.I.M.E., Vol. 215, p. 619.

14. SYKES, C. and BAMPFYLDE, J. (1934) Journal of the Iron and Steel Institute, Vol. 130, p. 389.

15. BENNET, W. D. (1952) Some Effects of Order-Disorder in Iron-Aluminum Alloys, Journal of the Iron and Steel Institute, Vol. 171-172, p. 372.

16. LAWLEY, A. and CAHN, R. J. (1961) Journal of Physics and Chemistry of Solids, Vol. 20, No. 3, p. 204.

17. SHMUELI, U. and RUDMAN, P., ASTIA Document No. 266327.

18. RAUSCHER, G. P. JR., (1962) A Study of the Superlattice Transformations in Iron-Aluminum Alloys, Thesis, University of Colorado.

19. LIPSON, J. (1950) Order-Disorder Changes in Alloys, Progress in Metal Physics, Vol. II, Bruce Chalmers, editor. Interscience Publishers, Inc. New York.

20. DIENES, G. J. and VINEYARD, G. H. (1957) Radiation Effects in Solids, Interscience Monographs in Physics and Astronomy, Vol. II, R. E. Marshak, Editor, Interscience Publishers, Inc., New York.

21. BILLINGTON, D. S. and CRAWFORD, J. H., JR. (1961) Radiation Damage in Solids, Princeton University Press, Princeton, New Jersey.

22. BISHAY, A. (1967) Interaction of Radiation With Solids, Adli Bishay, Editor, Proceedings of the Cairo Solid State Conference at The American University in Cairo, held September 3-8, 1966, Plenum Press, New York.

23. PENKOVSKII, V. V. (1964) Effect of Radiation on Metals, Elsevier Publishing Co., New York.

24. TOMA, R. F., JR. (1965) Order-Disorder in Fe_3Al at Various Temperatures Induced by Neutron Irradiation, Thesis, University of Missouri at Rolla.

25. SILSBEE, R. H. (1957) Journal of Applied Physics, Vol. 28 p. 1246.

26. SIEGEL, S. (1949) Effects of Neutron Bombardment on Order in the Alloy Cu,Au. Review of Physics, Vol. 75, p. 1823.

27. COOK, L. G. and CUSHING, R. L. (1953) The Effects of Neutron Irradiation in the NRX Reactor on the Order-Disorder Alloy Cu_3Au, Acta Metallurgy, Vol. 1, p. 539.

28. SEITZ, F. and KOEHLER, J. S. (1956) Displacement of Atoms During Irradiation, Solid State Physics (editors F. Seitz and D. Turnbull) Academic Press, Vol. 2, p. 307.

29. BRINKMAN, J. A., DIXON, C. E. and MEECHAN, C. J. (1954) Interstitial and Vacancy Migration in Cu_3Au and Copper, Acta Metallurgy, Vol. 2, p. 38.

30. KINCHIN, G. H. and PEASE, R. S. (1955) The Mechanism of the Irradiation Disordering of Alloys, Journal of Nuclear Energy, Vol 1. p. 200.

31. GLICK, H. L., WITZIG, W. F., BROOKS, F. C. and JOHNSON, W. E. (1952) Physics Review, Vol. 87, p. 1074.

32. GLICK, H. L. and WITZIG, W. F. (1953) Physics Review, Vol. 91 p. 236.

33. BLEWITT, T. H. and COLTMAN, R. R. (1952) Physics Review, Vol. 85, p. 389.

34. SAENKO, G. P. (1964) Effects of Neutron Irradiation on Order in Fe_3Al, Journal of Nuclear Materials, Vol. 11, 2, p. 220.

35. SEYBOLT, A. U., AIME Transactions, Vol. 218, 1960 p. 570-571.

36. ADAMS, J., and DUGDALE, R. A. (1952) Phil. Mag., Vol. 43, p. 1216.

37. KINCHIN, G. H. and PEASE, R. S. (1956) The Displacement of Atoms in Solid by Radiation, Review of Progress in Physics, Vol. 94, p. 1.

38. EDWARDS, D. R., Personal Communication

VITA

The author, Bruce Allan Betts, was born on August 17, 1938 in St. Louis, Missouri. He received his primary education at Baden and Ferguson, Missouri, and his secondary education at Ferguson, Missouri. He has received his college education from Southwest Baptist College, Bolivar, Missouri and University of Missouri - Rolla, Rolla, Missouri. He received an Associates of Arts Degree in Pre-Engineering from Southwest Baptist College in May, 1958 and a Bachelor of Science Degree in Metallurgical Engineering Nuclear Option from the University of Missouri School of Mines and Metallurgy in June, 1963.

He has been enrolled in the Graduate School of the University of Missouri - Rolla from September 1963 until October 1964, at which time he was employed as an experimental metallurgist at the Allison Division General Motors Corporation in Indianapolis, Indiana. Since September 1966 he has been enrolled in the Graduate School of the University of Missouri - Rolla. He is married and the father of two children.